# 2. THE TYRRHENIAN SEA BEFORE LEG 107[1]

J. P. Rehault[2], J. Mascle[2], A. Fabbri[3], E. Moussat[4], and M. Thommeret[2]

The Tyrrhenian Sea (Fig. 1) is a small triangular marine basin surrounded by Corsica, Sardinia, Sicily, and peninsular Italy, lying between the Neogene Western Mediterranean Basin and the Mesozoic Ionian and Levantine Basins (Biju Duval et al., 1978). The Tyrrhenian Sea has been, for more than a decade, the subject of many geophysical and geological explorations summarized by Morelli (1970), Boccaletti and Manetti (1978), Lort (1978), Moussat (1983), Duchesnes et al. (1986), and Rehault et al. (1984, 1987). The evolution of the Tyrrhenian Sea is unusual and intriguing in that the basin has developed both back of a subduction–volcanic-arc system (the Calabrian arc) and inside of successive collision zones (Alpine and Apennines s.l.). Collision is still active both east and south of the Tyrrhenian in the peninsular Apennines and Sicily. This evolution has resulted in the creation of a deep basin showing geophysical and petrological evidence of oceanic-type crust (crustal thickness, Moho depth, magnetic, gravity, heat flow, and related magmatism).

In this introduction we intend first to present a summary of the main geophysical data available today, second to illustrate the geological structures and sedimentary formations related to the recent evolution of the basin and, finally to provide a brief overview of the different geodynamic models which have been presented to explain the main characteristics of the Tyrrhenian Sea and surrounding area before Leg 107.

## MORPHOLOGY

The Tyrrhenian Sea consists of a deep central basin (sometimes termed bathyal plain) surrounded by narrow continental shelves and relatively steep continental slopes (Fig. 2). This discussion will cover the central basin first, then proceed counterclockwise around the continental margins from Sicily to Sardinia.

### Central Basin

The deep central basin is surrounded by the 3400-m isobath and reaches a maximum depth of 3600 m in its northwestern corner. In detail this very flat bottomed plain is dissected into numerous elongated north-northeast-trending small depressions, notably at the base of the Sardinian margin. The central plain can be divided into two main basins separated by a shallow sill (Fig. 1). The northwestern basin, the Magnaghi-Vavilov Basin contains two large submarine volcanoes (Fig. 3). The Magnaghi Volcano is located at the base of the Sardinian margin just east of a sublinear scarp called the Central Fault. The Vavilov Volcano, reaching a depth of 684 m, bisects the Magnaghi-Vavilov Basin. North-trending ridges bound the Vavilov Basin at the foot of the Sardinian margin (Monte de Marchi) and the Campanian margin (Monte Flavio Gioia). The southeastern basin, or Marsili Basin, is roughly rhombohedral in shape. The basin is bisected by the Marsili Seamount, the largest volcano within the Tyrrhenian Sea, culminating at 505 m. The Magnaghi, Vavilov, and Marsili volcanoes are tens of kilometers (30–50) in length. They are similarly elongated and subparallel with their long axis trending N10°–20°E.

### Continental Margins

The northern Sicily and western Calabria continental margins average 100–120 km in width. They are characterized by a system of close-spaced sediment-filled upper slope basins, the Cefalu, Gioia, and Paola Basins (Perityrrhenian Basins, Selli, 1970; Basin and Range System, Hsü, 1978). An arcuate belt of volcanoes known as the Eolian Islands follows the curve of the Sicily-Calabrian margin, about 60 km offshore. These islands have acted as structural dams for sediments being shed off the margins. A deep submarine canyon has formed around Stromboli Volcano, one of the most active volcanic islands.

Off Campania, northward to the latitude of Rome, the northwest-trending margin offers a similar configuration to the north Sicily and west Calabria margin. Upper slope basins are seen off Salerno and Napoli, segmented by northeast-trending bathymetric highs (Fig. 2). The Pontian Islands represent a volcanic archipelago in the vicinity of the Vesuvio Volcano. The lower slope includes a series of northeast- and northwest-trending highs. Toward the northwest (off Tuscany), in the northern Tyrrhenian, the Italian margin connects with the Corsica continental margin. This northern corner of the Tyrrhenian is characterized by a N10°E-trending fabric expressed by numerous horsts and grabens.

On the western side of the Tyrrhenian the continental margin widens appreciably, reaching its maximum width off Sardinia (about 250 km). As on the eastern and southern margins, the upper slope here also contains elongated sedimentary basins averaging 700 m in depth known as the Corsica-Sardinia Basins. To the east these basins are bounded by a series of linear highs; the most conspicuous ones are the Pianosa-Elba ridge (just south of Elba Island) and the Monte Baronie (off northeast Sardinia). The middle slope (Cornaglia Terrace) is rather flat, averaging 2500 m water depth. Toward the east, this flat domain is suddenly interrupted by a steep southeast-facing scarp, the Central Fault, trending N30°E, with about 1000 m of relief (Fig. 3). The lower continental slope, between 3200 and 3400 m, is cut by a series of elongate depressions and sublinear asymmetric highs (trending N10°–30°E) suggesting tilted block morphology.

## GRAVITY

The Bouguer anomaly gravity map of Figure 4 is a compilation of data from Morelli (1970) and Morelli and Finetti (1973) for the Tyrrhenian Sea, from Colombi et al. (1973) for Sicily and peninsular Italy, from Bayer (1977) for Corsica, and from Morelli (1975) for Sardinia.

Two prominent positive anomaly areas (more than 200 mgal) are clearly seen on the map, characterizing the northwestern part of the Ionian Sea and the central Tyrrhenian Sea. These two areas are separated by an arcuate belt of negative anomalies notably in Sicily and in peninsular Italy. These negative values

[1] Kastens, K. A., Mascle, J., Auroux, C., et al., 1987. *Proc., Init. Repts.* (*Pt. A*), *ODP*, 107.

[2] Laboratoire de Géodynamique sous Marine Université Paris VI, CNRS, BP 48, 06230 Villefranche sur Mer, France.

[3] Instituto di Geologia Marina, CNR, Via Zamboni 65, Bologna, Italy.

[4] IFREMER, Centre de Brest, BP 337, 29273 Brest, France.

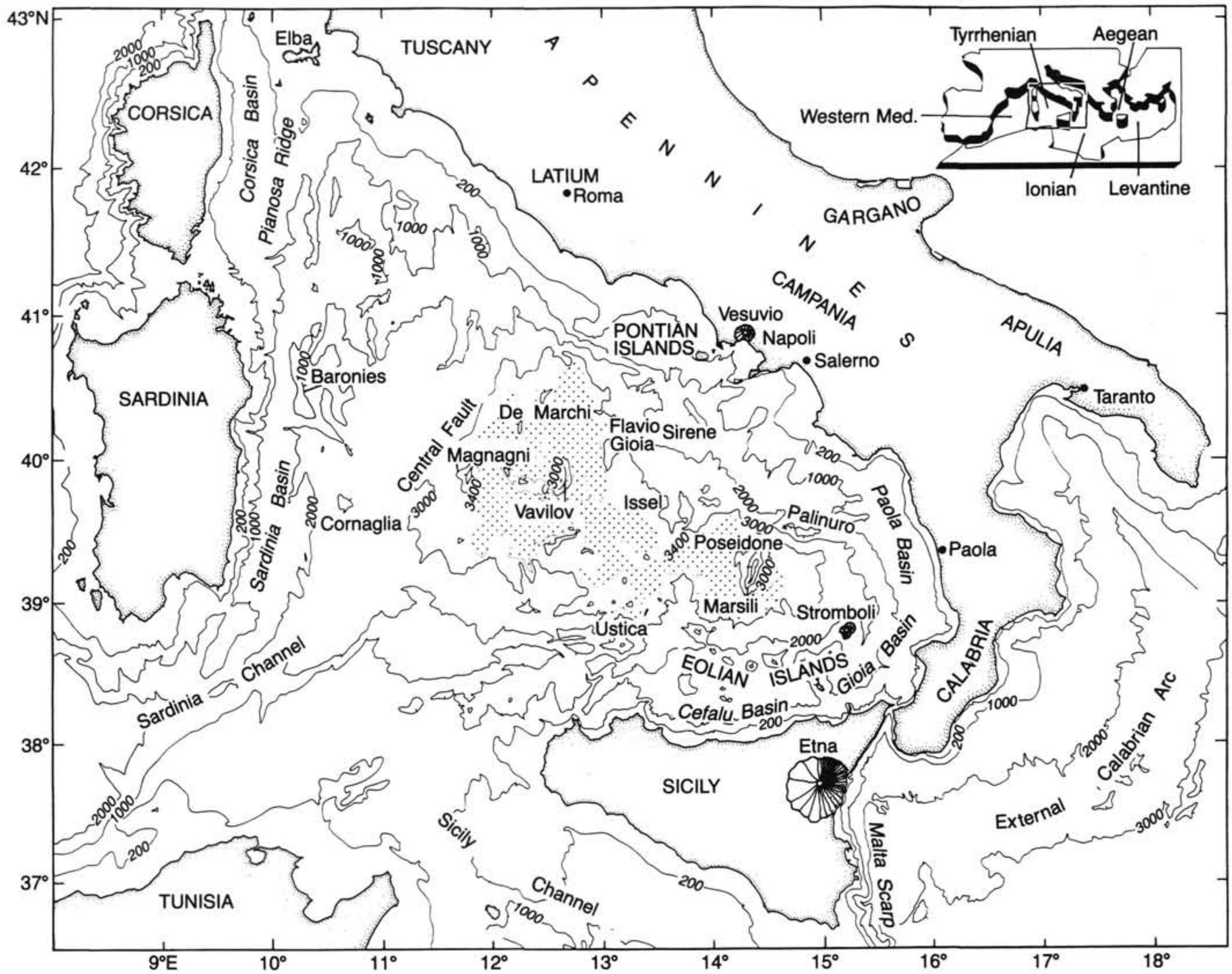


Figure 1. Simplified bathymetry of the Tyrrhenian areas (200-, 1000-, 2000-, and 3000-m bathymetric lines). The deep central basin (dotted) is outlined by the 3400-m isobath. The toponymy used in the text is also given.

coincide with sedimentary basins caught up in the orogenic belts (Caltanisseta Basin in Sicily and Bradanic Trough in southern Italy). In the region of Calabria the arc of negative anomalies lies offshore, in the external Calabrian Arc (Rossi and Sartori, 1981). The gravity lows off Calabria are of lower amplitude and discontinuous.

Within the Tyrrhenian Sea itself we observe a regular increase of the anomalies from the margin toward the center of the basin. High values, greater than 200 mgal, delineate the bathymetric bathyal plain. Values greater than 250 mgal are found only within the small deep sub-basins surrounding the Vavilov and Marsili seamounts, although the volcanoes themselves are associated with anomalies less than 250 mgal. This may indicate that they are isostatically not yet compensated, suggesting thus a rather young age.

## CRUSTAL STRUCTURE—LITHOSPHERE THICKNESS

Numerous refraction data have been obtained within the Tyrrhenian Sea (Duchesnes et al., 1986 and references therein). The sketch map of Figure 5 shows the depth of the Moho unconformity according to a synthesis of all available data. The most significant observation relates to the occurrence of two restricted domains where the Moho depth is less than 10 km, giving a crustal thickness of less than 7 km. As seen by comparison with the bathymetric map, these two domains are respectively superimposed on the Magnaghi-Vavilov Basin and on the Marsili Basin. A crustal bridge about 15–17 km thick separates the two basins (Steinmetz et al., 1983). Between the Magnaghi-Vavilov Basin and the Sardinia-Corsica block, we notice a steep transition between a crust less than 7 km thick and a normal continental crust, about 30 km thick over a distance of 200 km. In parallel with the overall thinning of the crust, we can observe the disappearance of the 6.0 km/s layer ("granitic" layer) toward the central basin (Fig. 6). Within the Magnaghi-Vavilov Basin, the seismic velocity distribution indicates an oceanic-type crust. The underlying mantle is characterized by $P_n$ velocities lower than typical oceanic mantle, 7.75–7.80 km/s (Recq et al., 1984; Duchesnes et al., 1986).

Under the central Ionian Sea, the Moho is well documented at 20 km depth (Finetti, 1982). The Moho then dips northwestward beneath the external Calabrian arc reaching 35 km depth immediately southeast of Calabria. Under southern Italy, the situation is complex, but Morelli et al. (1975) and Schütte (1978) have interpreted seismic refraction experiments to indicate crustal superposition: an upper Tyrrhenian-Calabrian Moho between 15 and 20 km lies over a lower Ionian Moho about 40 km deep.

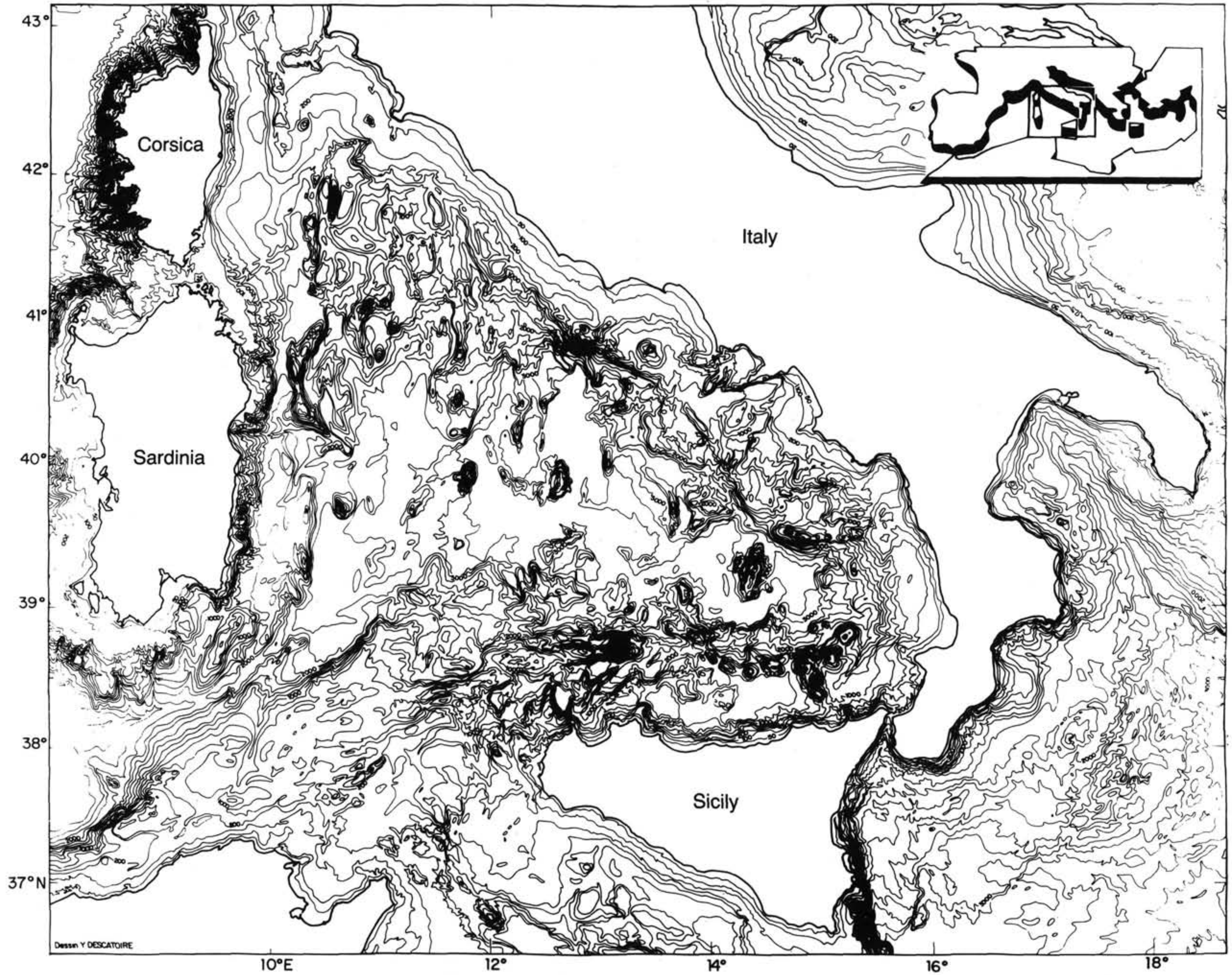


Figure 2. General bathymetry of the Tyrrhenian Sea and surrounding areas from international bathymetry chart of the Mediterranean Intergovernmental Oceanographic Commission (UNESCO, 1981). Contour interval: 200 m.

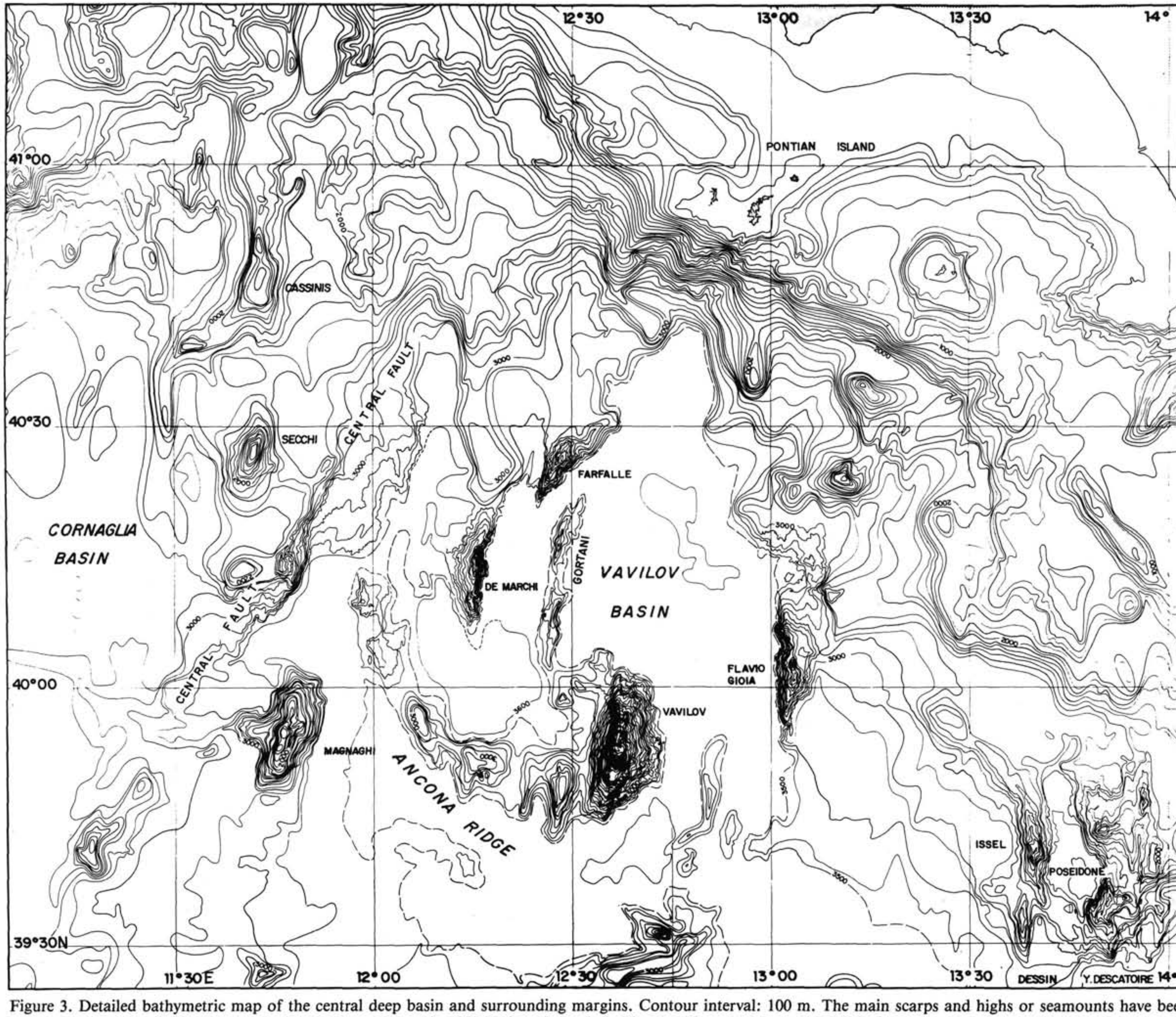


Figure 3. Detailed bathymetric map of the central deep basin and surrounding margins. Contour interval: 100 m. The main scarps and highs or seamounts have been mapped using a detailed multibeam bathymetric survey run in 1982 on board the *Jean Charcot*. Note the asymmetry of the lower margin mounts, notably the Monte de Marchi and Flavio Gioia bathymetric highs.

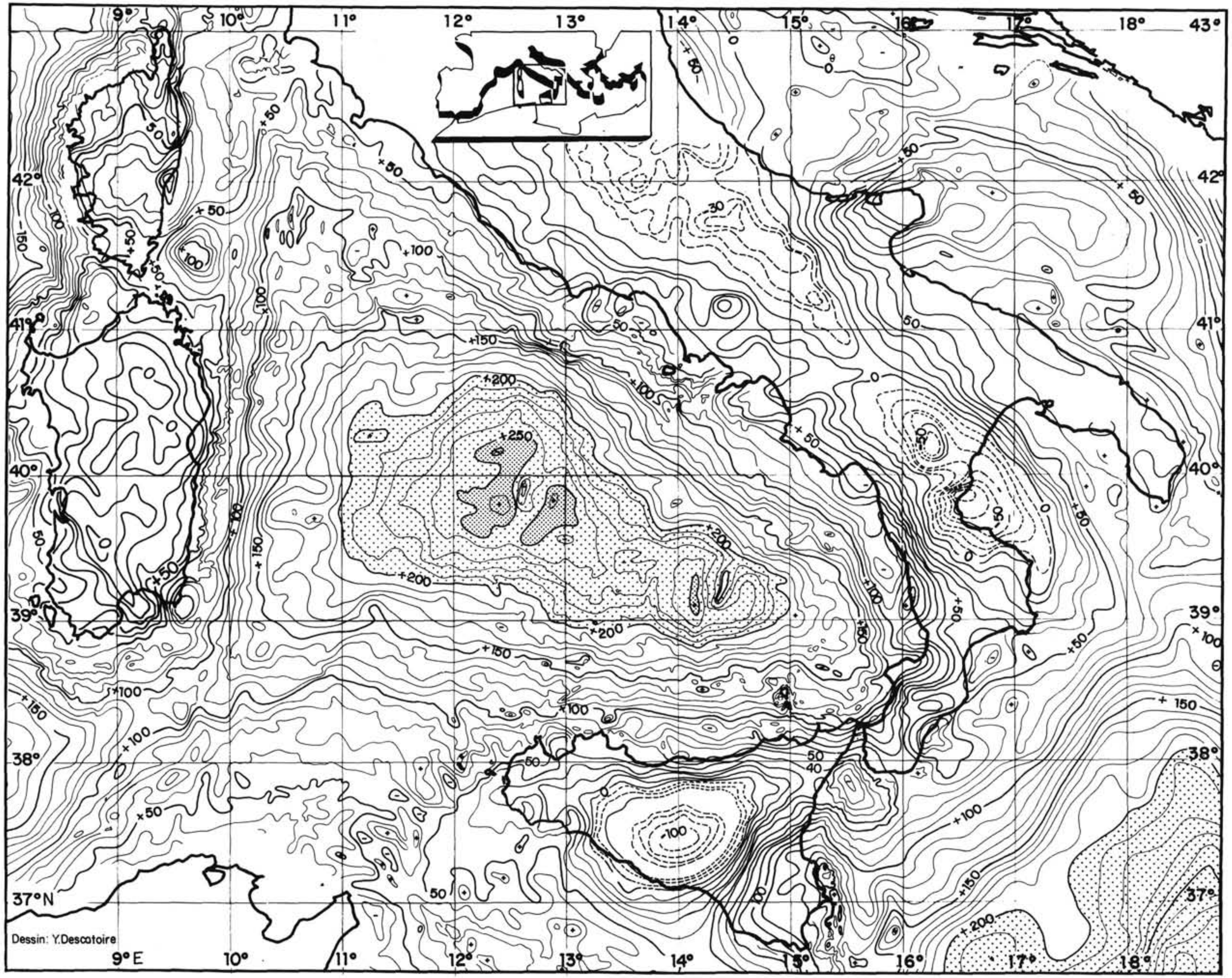


Figure 4. Gravity map (Bouguer anomaly) of the Tyrrhenian Sea and surrounding areas. Contour interval: 10 mgal. This map is a compilation of data from Morelli (1970, 1975), Columbi et al. (1973), and Bayer (1977). Values higher than 200 mgal are dotted; negative values are shown as dashed lines.

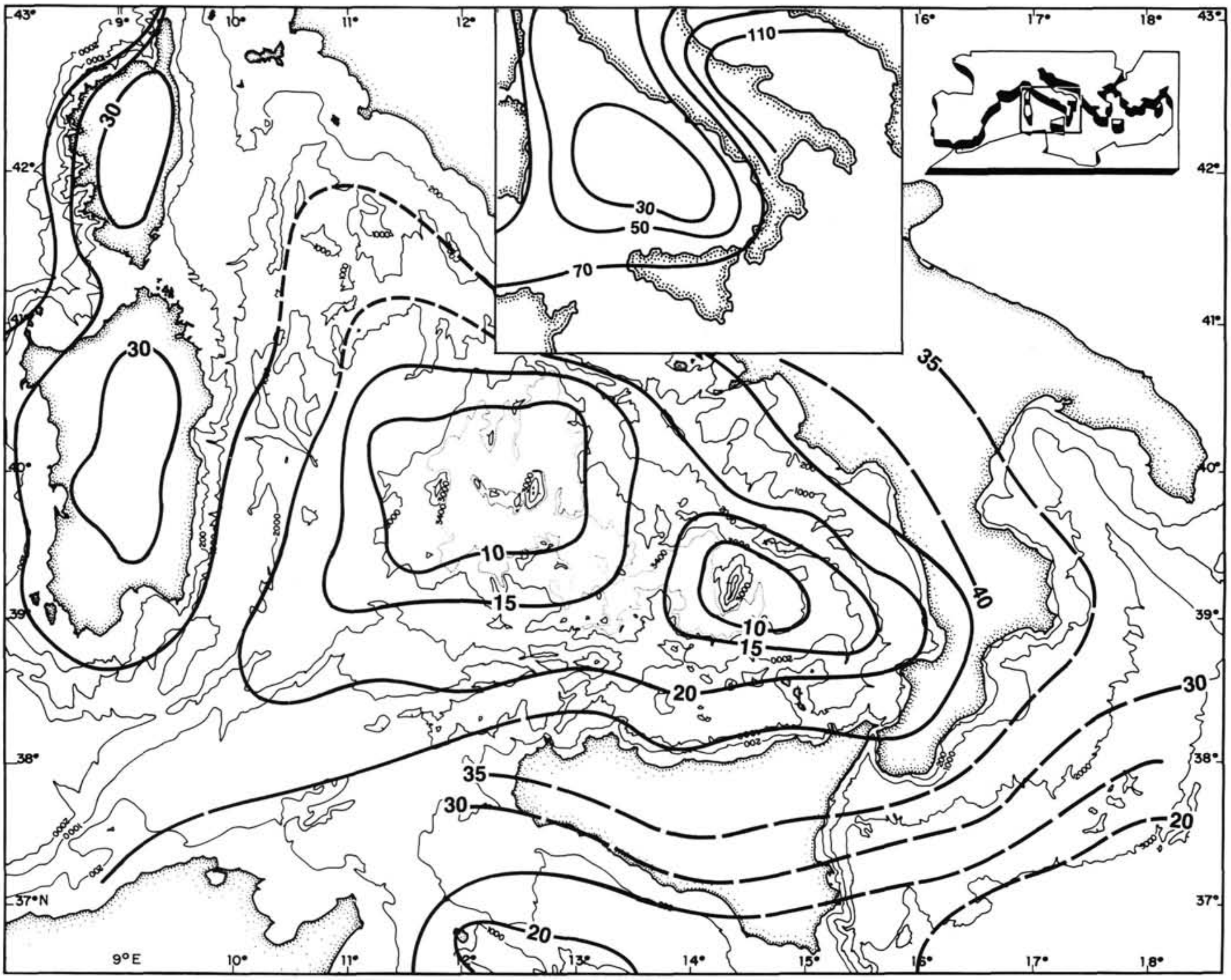


Figure 5. Moho depth (km below sea level) beneath the Tyrrhenian Sea and surrounding areas simplified from Nicolich (1981), Steinmetz et al. (1983), Boccaletti et al. (1984), Recq et al. (1984), and Duschenes et al. (1986). Moho depth of the Ionian-Apulian area is shown as dashed lines. In inset, thickness of the lithosphere (km) after Panza et al. (1980).

Rayleigh wave dispersion analysis (Panza and Calcagnile, 1979) for the Tyrrhenian area indicates that the shallow Moho is linked to a marked thinning of the entire lithosphere. Beneath the central plain the lithosphere's total thickness is less than 30 km (Fig. 5, inset). This observation is in good agreement with the high value of the gravity anomalies.

## THERMAL REGIME

More than 200 surficial heat flow stations (Fig. 7) are available within the Tyrrhenian Basin (Erickson, 1970; Erickson and Von Herzen, 1978; Zolotarev and Sochel'nikov, 1980; Della Vedova et al., 1984; Hutchison et al., 1985). Data from these stations define several heat flow provinces. The thermal regime of the upper to middle margin (except off Tuscany) is characterized by low values (less than 100 mW/m$^2$). In contrast, the central Tyrrhenian has values higher than 150 mW/m$^2$ reaching local maxima greater than 200 mW/m$^2$ within the Vavilov and the Marsili Basins.

Along peninsular Italy the heat flow values distribution is complex, including two "hot" provinces. The first is just off Tuscany associated with recent volcanic activities. The second lies at the base of the Campania margin, superimposed on the Palinuro volcanic fault zone, where heat flow values in excess of 1000 mW/m$^2$ have been measured (Della Vedova et al., 1984).

Within the central basin we observe several local anomalies in the regional heat flow distribution. For example, around the Vavilov and Marsili volcanos, low values (0–20 mW/m$^2$) alternate with very high heat flow values (as high as 300 mWm$^2$) in a distance of less than 15 km. These phenomena are interpreted in relation to hydrothermal circulations; both volcanoes are thinly sedimented and consequently experience rapid cooling through fractured lava flows.

Regional high heat flow isotherms are in good agreement with both positive Bouguer anomalies and with shallow Moho depth areas.

## MAGNETISM

The map shown on Figure 8 is derived from a general aeromagnetic map of the Italian area (AGIP, 1981) with the exception of Corsica (Galdeano and Rossignol, 1977). The anomalies shown are drawn from residual-field anomalies and are therefore only relative.

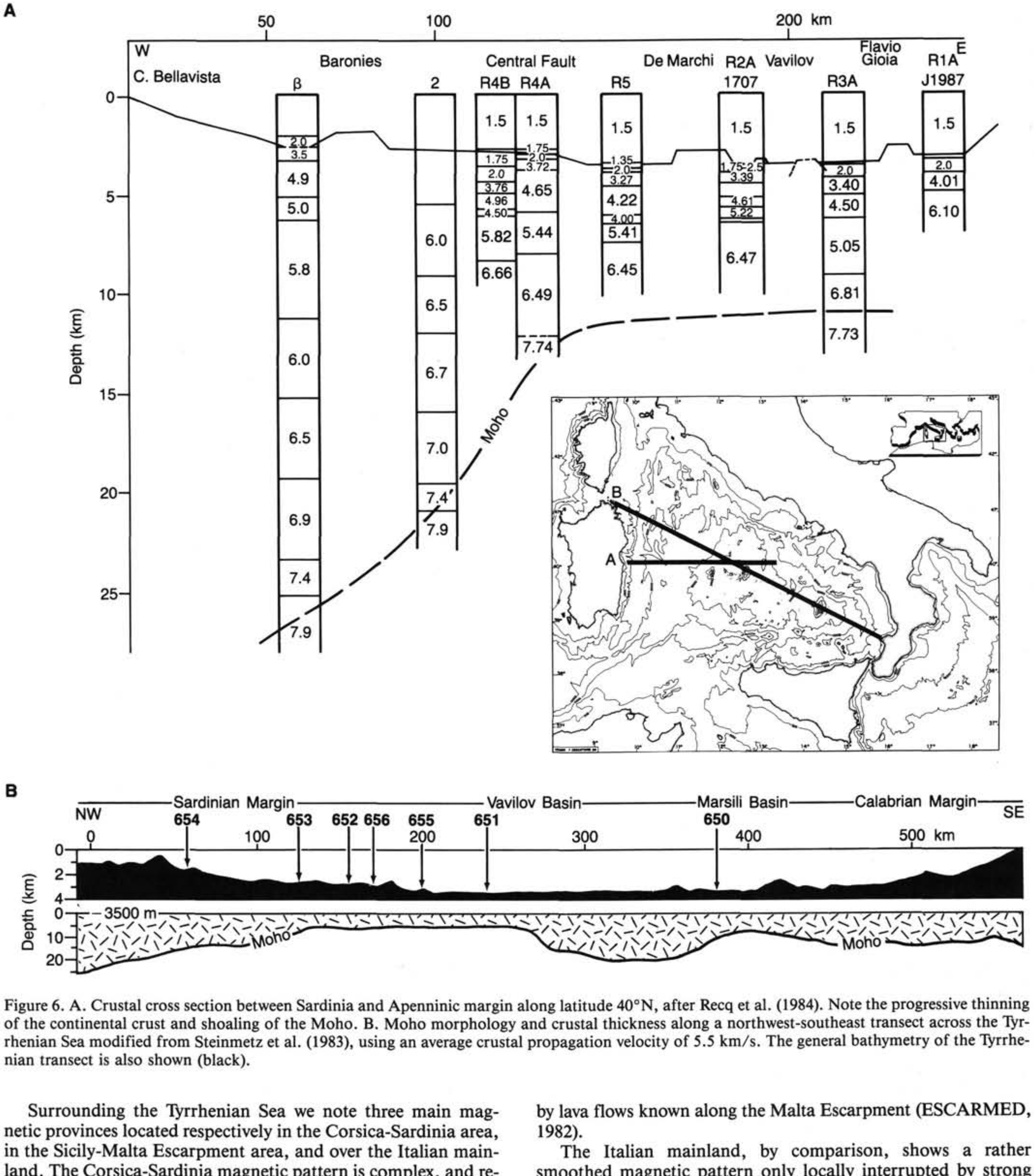


Figure 6. A. Crustal cross section between Sardinia and Apenninic margin along latitude 40°N, after Recq et al. (1984). Note the progressive thinning of the continental crust and shoaling of the Moho. B. Moho morphology and crustal thickness along a northwest-southeast transect across the Tyrrhenian Sea modified from Steinmetz et al. (1983), using an average crustal propagation velocity of 5.5 km/s. The general bathymetry of the Tyrrhenian transect is also shown (black).

Surrounding the Tyrrhenian Sea we note three main magnetic provinces located respectively in the Corsica-Sardinia area, in the Sicily-Malta Escarpment area, and over the Italian mainland. The Corsica-Sardinia magnetic pattern is complex, and reflects the local geology. Magnetic anomalies are associated with the Permian volcanoes, the ophiolitic suture of Alpine-Corsica, the Neogene to Pleistocene volcanics of Sardinia, and the magmatic-plutonic system of the Elba-Monte Cristo ridge. In Sicily and along the northern Malta Escarpment, the magnetic anomalies are well explained by Etna volcanics (positive anomaly) and by lava flows known along the Malta Escarpment (ESCARMED, 1982).

The Italian mainland, by comparison, shows a rather smoothed magnetic pattern only locally interrupted by strong anomalies superimposed on the Pliocene-Pleistocene volcanic provinces (Vesuvio-Pontian Islands, Flegrean Fields; Latium and Tuscany Province; see "A Review of Circum-Tyrrhenian Regional Geology" chapter, this volume).

Within the Tyrrhenian Sea itself we observe a contrast between the central plain with strong magnetic anomalies and most

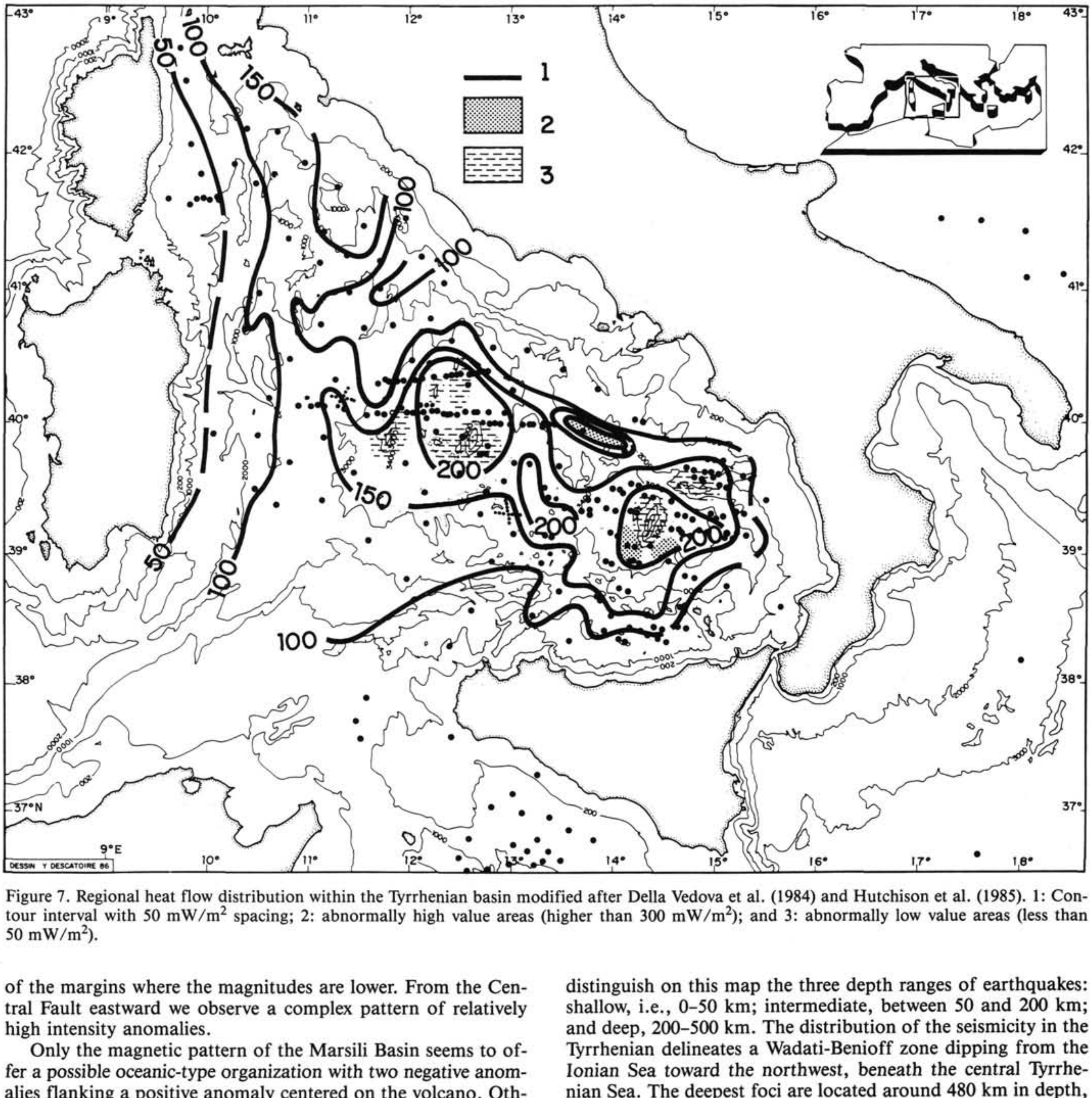


Figure 7. Regional heat flow distribution within the Tyrrhenian basin modified after Della Vedova et al. (1984) and Hutchison et al. (1985). 1: Contour interval with 50 mW/m$^2$ spacing; 2: abnormally high value areas (higher than 300 mW/m$^2$); and 3: abnormally low value areas (less than 50 mW/m$^2$).

of the margins where the magnitudes are lower. From the Central Fault eastward we observe a complex pattern of relatively high intensity anomalies.

Only the magnetic pattern of the Marsili Basin seems to offer a possible oceanic-type organization with two negative anomalies flanking a positive anomaly centered on the volcano. Otherwise, it has not been possible to identify Vine-Matthews type lineated anomalies in the Tyrrhenian. However, Moussat (1983) believes that anomalies are distributed following two main trends: the first N10°-30° direction, relatively well evidenced along the Central Fault and within the Marsili Basin and possibly seen over the Vavilov area; the second N110°-120°, less obvious direction offsets the previous trend in the Central basin but is well expressed by intense lineaments at the foot of the Northern Sicilian margin and along the Sardinian margin, South of Baronie Mounts.

## SEISMICITY

Figure 9 is a compilation of earthquake distribution within the Italian area between 1962 and 1982 with a few additional recent points (Ritsema et al., 1969; Gasparini et al., 1982). We distinguish on this map the three depth ranges of earthquakes: shallow, i.e., 0-50 km; intermediate, between 50 and 200 km; and deep, 200-500 km. The distribution of the seismicity in the Tyrrhenian delineates a Wadati-Benioff zone dipping from the Ionian Sea toward the northwest, beneath the central Tyrrhenian Sea. The deepest foci are located around 480 km in depth, just beneath the eastern Vavilov Basin. Early works (Caputo et al., 1972; Panza et al., 1979) suggested that the Benioff zone was discontinuous, as might be produced by a disconnected or broken slab. Using additional stations in the recording network, Gasparini et al. (1982) have shown the continuity of the Benioff zone. The "spoon" shape of the Benioff zone (Fig. 9) has been attributed to deformation of the downgoing Ionian plate where it is locked between the continental crust of Sicily and Apulia.

In addition, analysis of earthquake focal mechanisms indicates a generally extensional stress field both for the Tyrrhenian Sea and Calabria, together with strike-slip components (Ghisetti and Vezzani, 1981; Gasparini et al., 1982; Moussat et al., 1985, 1986; Boccaletti et al., 1984). Compressional events characterize both the Sicilian and Apenninic borders, coinciding with the northern and southwestern extremities of the main thrust zones

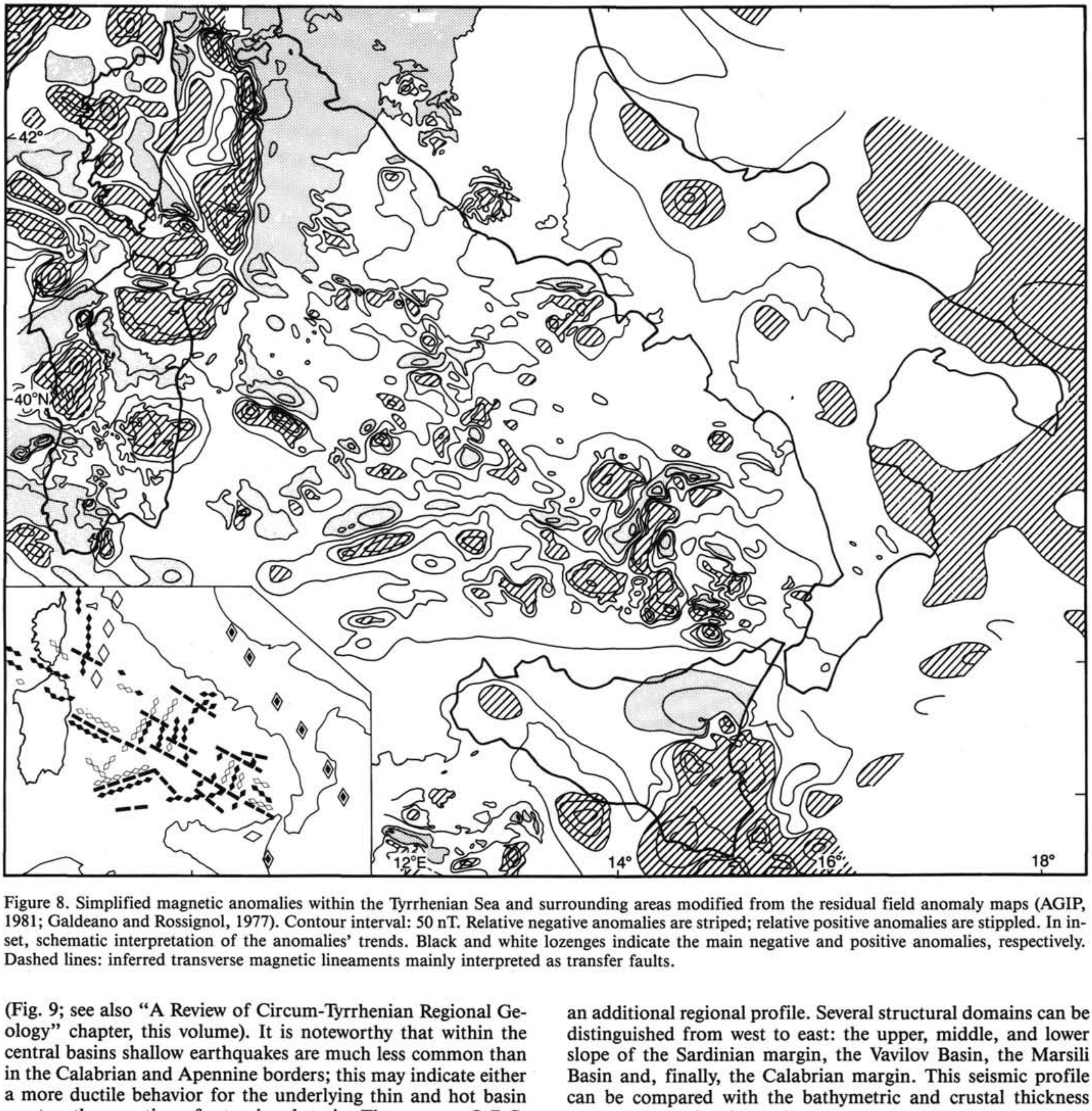


Figure 8. Simplified magnetic anomalies within the Tyrrhenian Sea and surrounding areas modified from the residual field anomaly maps (AGIP, 1981; Galdeano and Rossignol, 1977). Contour interval: 50 nT. Relative negative anomalies are striped; relative positive anomalies are stippled. In inset, schematic interpretation of the anomalies' trends. Black and white lozenges indicate the main negative and positive anomalies, respectively. Dashed lines: inferred transverse magnetic lineaments mainly interpreted as transfer faults.

(Fig. 9; see also "A Review of Circum-Tyrrhenian Regional Geology" chapter, this volume). It is noteworthy that within the central basins shallow earthquakes are much less common than in the Calabrian and Apennine borders; this may indicate either a more ductile behavior for the underlying thin and hot basin crust or the cessation of extensional strain. There are no O.B.S. microseismicity data available to distinguish between the hypotheses.

## SHALLOW STRUCTURE AND SEISMIC STRATIGRAPHY

Figures 10A and B show most of the seismic reflection data tracklines available within the Tyrrhenian Sea. Most of these are single channel seismic lines recorded using a sparker or an airgun seismic source (I.G.M. *Bologna* and L.G.S.M. *Villefranche*, respectively); multichannel seismic (MCS) lines, from O.G.S. *Trieste*, are also indicated, as well as site survey lines made for Leg 107.

Figure 11 (back pocket) shows a condensed seismic section across the Tyrrhenian Basin from the Sardinian margin to the Calabrian margin. The reader is referred to Morelli (1970) for an additional regional profile. Several structural domains can be distinguished from west to east: the upper, middle, and lower slope of the Sardinian margin, the Vavilov Basin, the Marsili Basin and, finally, the Calabrian margin. This seismic profile can be compared with the bathymetric and crustal thickness transect shown in Figure 6B.

### The Upper Sardinian Margin

The upper slope (between 200 and 1700 m) is dissected by numerous east-trending canyons and north-trending basement ridges (Fig. 2). Off northern Sardinia we observe a slope basin (the Sardinia Basin) partially filled with ponded sediment and bounded to the east by north-trending basement ridges (Fig. 12). The largest of these ridges is the Monte Baronie (Fig. 1) from which sediments of continental lithology have been dredged (Colantoni et al., 1981). These bordering highs appear as symmetrical horst structures, and as asymmetrical blocks tilted either landward or seaward (Fig. 13).

Within the Sardinia basin, the following lithoacoustic sequences have been described from the top to the bottom (Fabbri and Curzi, 1979; Moussat, 1983): (1) A series of well-layered

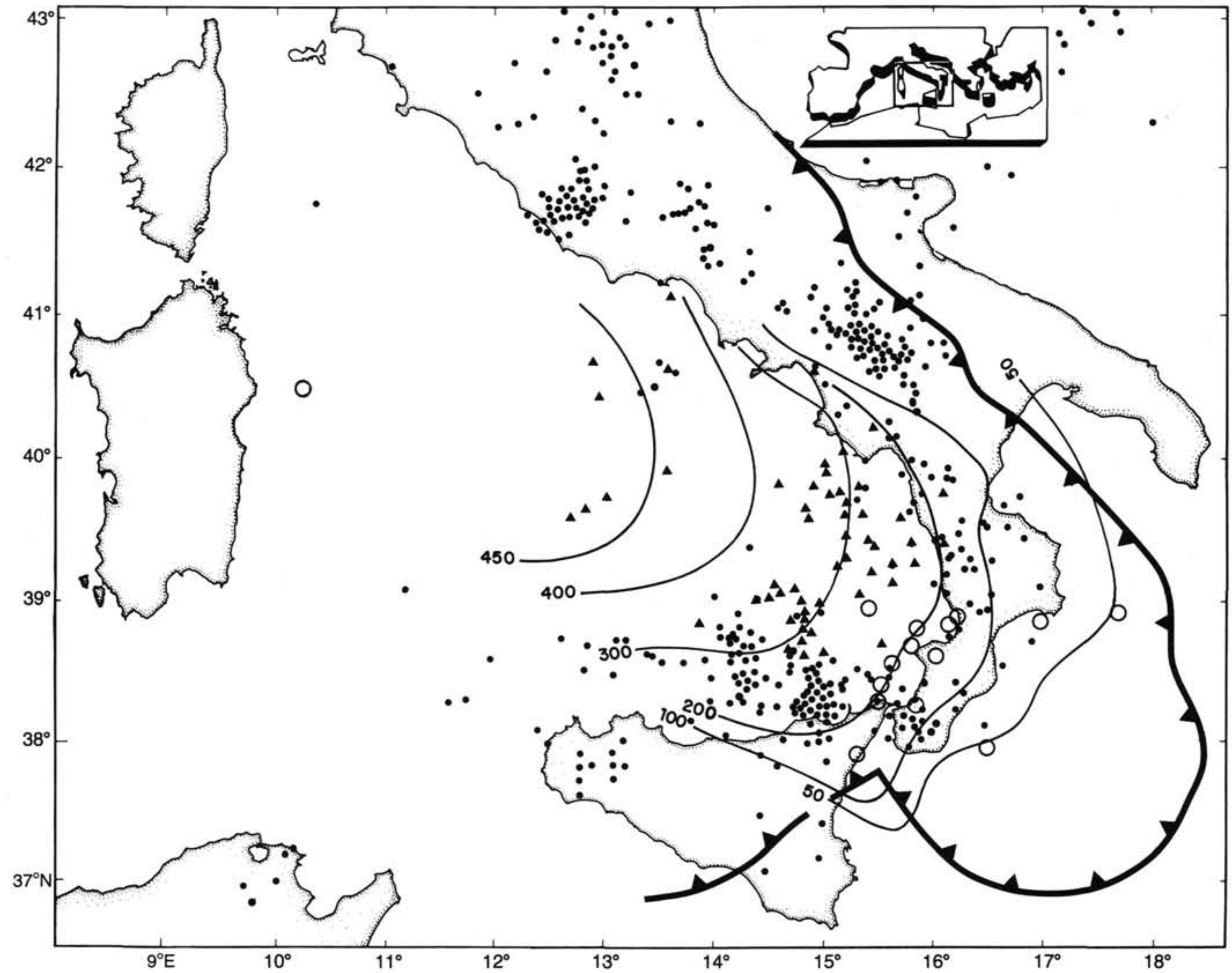


Figure 9. Seismicity of the Tyrrhenian domain, mainly from the Cambridge catalog until 1982. Shallow earthquakes (0–50 km), black dots; intermediate earthquakes (50–200 km), white circles; and deep earthquakes (200–500 km), black triangles. Depths of the Benioff Zone in kilometers are simplified after Gasparini et al. (1982). The main thrust fronts of Apennines, Sicilides, and external Calabrian are also indicated.

seismic reflectors filling the basin with variable thickness (as much as 1 s twtt) and interpreted as onlapping Pliocene-Pleistocene turbidites. This sequence is dammed to the east by bordering structural highs. Under the ponded turbidites, we observe either a highly diffractive seismic surface or an intermediate acoustic unit (2) characterized by a strongly reflective upper surface. The diffractive surface, where present, has been interpreted as a late Miocene (Messinian) erosional surface or as a terrigenous (locally deltaic) deposit, also of Messinian age. The intermediate unit with strongly reflective upper surface has been interpreted as thin Messinian evaporites. (3) A lower seismic unit comprises conformable well-layered seismic reflectors. Finally, the deepest detected seismic unit (4) represents either a true acoustic basement or deeper highly deformed sedimentary strata. Units 3 and 4 were inferred to be respectively of Tortonian age and of Oligocene-Miocene age (Fabbri and Nanni, 1980; Rehault et al, 1987).

## The Middle Sardinian slope (including Cornaglia Terrace)

The western side of the middle slope contains several north-trending basement ridges. On several ridges (Fig. 14), a history of tilting has been inferred from the geometry of the seismic units (Rehault et al., 1987): subparallel dipping reflectors at depth are inferred to represent pre-rift sediments of unknown age; an overlying dipping wedge of sediments, estimated to be from middle to late Miocene, is considered syn-rift; and a surficial unit of subhorizontal reflectors referred to as Pliocene-Pleistocene is thought to have been deposited post-rift.

The eastern portion of the middle slope is a wide (>100 km) flat domain called Cornaglia Terrace. In this region, DSDP Site 132 documented a nearly-complete hemipelagic Pliocene-Pleistocene section about 200 m thick (Ryan, Hsü, et al., 1973). The Miocene/Pliocene boundary corresponds to a strong acoustic reflector (the M-reflector of Ryan, 1973, and the Y-reflector of Selli and Fabbri, 1971), which marks the top of Messinian evaporites (Ryan, Hsü, et al., 1973). Thickness in excess of 800 m of Messinian evaporites (the maximum thickness of this formation within the Tyrrhenian basin) have been inferred in this area, where we also note the presence of numerous diapiric structures (Curzi et al., 1980).

Toward the east the Cornaglia Terrace is abruptly bounded by a series of east-facing scarps trending N30° constituting the Central Fault (Selli and Fabbri, 1971). The seafloor steps down more than 1000 m from the middle margin to the lower margin across the fault zone. Toward the south the relief of the Central Fault system progressively decreases, but the feature is still expressed by a series of small-amplitude structural highs and scarps (Fig. 15).

Numerous piston cores and dredge stations have been occupied along the Central Fault scarps; they have provided a stratigraphic succession including late Miocene to Pleistocene sediments together with fragments of limestones and metamorphic rocks interpreted as pieces of the Sardinian basement (Fabbri et al., 1980; Colantoni et al., 1981). Observations made during dives by the submersible *Cyana* in this area (Gennesseaux et al., 1986) show a stair-case morphology and brecciated deposits suggestive of normal fault activity.

### The Lower Sardinian Margin

At the foot of the main Central Fault scarp lies another relatively flat area. This domain is characterized by a system of narrow basins and structural blocks trending on average N10°E (Figs. 2 and 16). Some of these structural blocks are overlain by dipping and wedging seismic units; as on the upper Sardinian margin, these units have been interpreted in terms of tilting of fault-bounded blocks (Moussat et al., 1984; Rehault et al., 1984, 1987) (Fig. 17). The surficial, flat-lying reflectors have been interpreted as Pliocene-Pleistocene turbidites. The thickness of the inferred Pliocene-Pleistocene sequence is highly variable because of turbidite ponding amid the structural complexities of the basement relief. There is no seismic indication of typical evaporitic Messinian acoustic facies. Therefore the sequences under the "M" reflector have been attributed to pre-Messinian (Tortonian to Oligocene-Miocene) strata submitted to erosion during the Messinian (Moussat et al., 1984; Rehault et al., 1987). This was considered as an indication that during late Miocene time this lower margin area was in a higher position than the Cornaglia Terrace.

The Monte de Marchi and its neighbor, the Monte Farfalle (Fig. 3), are the largest tilted basement blocks, standing as much as 1.4 km above the surrounding ponded turbidites. This high-standing ridge (Fig. 18) lies just west of the inferred transition from continental to oceanic-type Vavilov Basin crust. It has been proposed (Rehault et al., 1987) that de Marchi and Farfalle represent one previously continuous ridge which has been offset by an east-trending right-lateral strike slip fault. Dredging and submersible dives along the steep eastern slopes of Monte de Marchi have recovered phyllites, greenschists, metabasalts, and radiolarites (Colantoni et al., 1981). By analogy with circum-Tyrrhenian outcrops, these rocks have been inferred to be of Hercynian and Alpine origin. These basement rocks are cut by N10°–30°E subvertical major fault scarps and transverse (N110°–140°E) subtle open fractures (Gennesseaux et al., 1986).

### The Vavilov Basin

Vavilov Basin is a flat-floored triangular-shaped basin, with water depths greater than 3500 m (Fig. 2). Monte de Marchi (Fig. 18) and Farfalle to the west, Flavio Gioia to the east, Vavilov Volcano to the south, and a series of seamounts known as the D'Ancona Ridge to the southwest constitute the boundaries of the basin. A subdued elongate basement ridge (Gortani Ridge) parallels the western edge of the basin (Figs. 3 and 19). Seismic profiles show that the elongate ridge consists of high-velocity basement (velocity of 5.2 km/s) just covered by a thin sedimentary layer.

On seismic records the Vavilov plain appears as a thickly sedimented basin with a sedimentary fill made of flat-lying and well-reflecting units attributed to Pliocene-Pleistocene turbiditic sediments (Fig. 19, back pocket). Several slight angular unconformities are detected within these sequences. These unconformities have been tentatively correlated with several tectonic events occurring around the Tyrrhenian Sea (Moussat et al., 1984). Below the inferred Pliocene-Pleistocene deposits, chaotic acoustic sequences have been locally observed and attributed either to pericontinental or fluviatile deposition (Malinverno et al., 1981) or to late Miocene volcaniclastics (Moussat et al., 1984).

The map of Pliocene-Pleistocene sedimentary thickness in the Vavilov basin (Fig. 20) indicates that an elongated and segmented basement high extends northward in apparent continuity with the Vavilov Volcano. This N10°E series of structural highs has been interpreted as an aborted accretionary center developing at the axis of the Vavilov rift system (Rehault et al., 1987).

DSDP Site 373, located on a small N10°E-trending ridge southeast of Vavilov Volcano (Fig. 20), yielded oceanic-type tholeiites (Dietrich et al., 1978; Barberi et al., 1978). Dredged stations along the Vavilov Volcano as well as on the Magnaghi Seamount just to the west have yielded transitional-type basalts (Selli, 1970; Fabbri and Selli, 1977) dated around 2.7 Ma for Magnaghi Seamount. Lava flows have been observed and sampled during submersible dives along Vavilov Volcano; these flows are also made of transitional-type basalt as young as 0.5 Ma (Gennesseaux et al., 1986b). These basalts seem to have been recently faulted.

### The Lower Apenninic Margin

Like the Sardinian margin, the lower Apenninic margin is bounded by asymmetric highs, Monte Flavio Gioia (Figs. 2 and 19) and other less prominent ridges. On Flavio Gioia, continental rocks have been observed during submersible dives and obtained by dredging (Dal Piaz et al., 1983). Little is known about this portion of the Apenninic margin. However, the water depth of 2500 m, the presence of thickly sedimented basins, and the inferred presence of Messinian evaporites, suggest an analogy with the Cornaglia Terrace on the conjugate Sardinian margin.

Distensive features, locally injected by magmatism, cut across the upper-middle margin; they present a general trend oriented north-south to northwest-southeast. For example, the prominent linear N140°E feature, on the upper slope off Naples, has been interpreted as one of the margin blocks, slightly overthrusting westward due to local transpression related to the progressive southeastward opening of the basin (Fig. 19B).

### The Marsili Basin and Surrounding Margins

The second of the two deep Tyrrhenian Basins, the Marsili Basin, is found southeast of the Vavilov Basin, surrounded by the margins of Campania, Calabria, and Northern Sicily (Figs. 1 and 2).

### The Campanian Margin

South of Salerno, the continental margin appears controlled by two main structural trends: a west-northwestward direction is defined by elongated scarps and highs in the vicinity of the Palinuro Seamount; northeast trends are expressed in a series of basement highs, scarps, and linear canyons inferred to be fault controlled. This structural grid closely controls the shape of the Campanian coastline such as in the bays of Salerno and Policastro for example (Figs. 1 and 2). Recent extensional tectonics are apparent from seismic data, as for example off Policastro (Fig. 21). The slope promontory which forms the thick-crusted bridge between Vavilov and Marsili Basins is itself faulted into a series of horsts, including Monte Issel and Monte Poseidone. The eastern face of Monte Poseidone (western boundary of Marsili Basin) has a stair-case morphology with westward-tilted reflectors (Fig. 22).

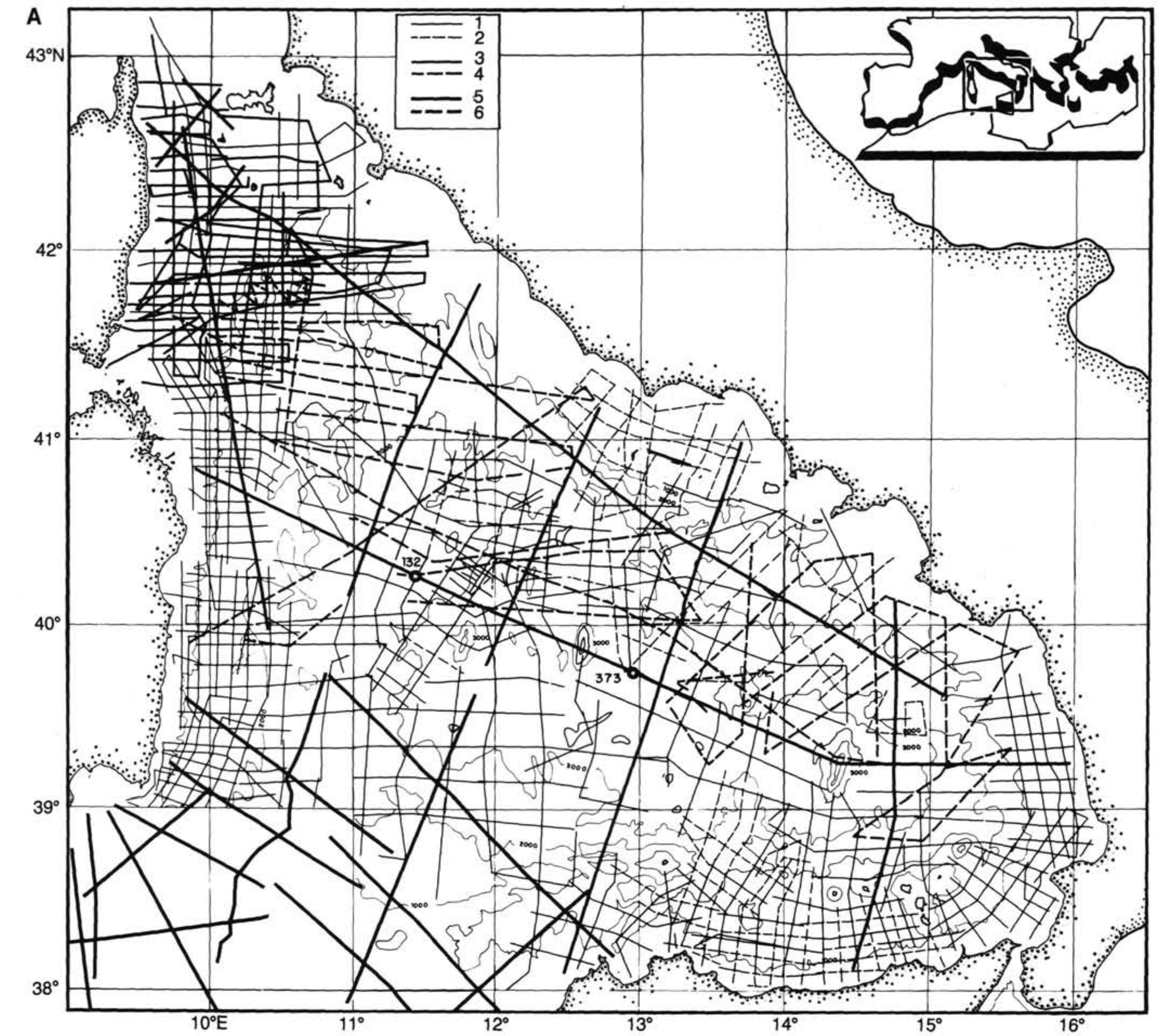


Figure 10. A. Available seismic lines in the Tyrrhenian Sea before Leg 107 from various sources. 1–4: single channel lines from IGM *Bologna* and LGSM *Villefranche sur Mer* (1970–84); 5–6: multichannel lines from OGS *Trieste* (1970-80). B. Track lines of the multichannel site survey made for Leg 107 (March 1985), IFP, IFREMER, CNRS. Two water-gun "Sodera"-shots spacing 25 m or 50 m—IFP-AMG Streamer, 48 channels; IFP processing.

## The Calabrian Margin

Off western Calabria, the margin is characterized by the presence of upper slope basins (the Paola and Gioia Perityrrhenian Basins) with a ponded sediment sequence (as thick as 5 km) inferred to be Pliocene-Pleistocene turbidites (Fig. 23) (Barone et al., 1981). To the west these basins are bounded by structural highs which may correspond to large-scale tilted blocks. The Paola and Gioia basins are believed to result both from extensive evolution originating in the late Miocene and from vertical isostatic adjustments to sediment loading. The influx of terrigenous sediment has been rapid and voluminous because of the uplift of Calabria (Schutte, 1978; Moussat, 1983).

This complex evolution has resulted in the presence of several unconformities (Fig. 23) within the basin sedimentary fill, the last one of uppermost Pleistocene times (Fabbri et al., 1981).

## The Northern Sicilian Margin

Comparable slope basins extend along the upper Sicilian margin (e.g., the Cefalu Basin and western part of Gioia Basin) (Fig. 23). These basins seem to have resulted from a similar rifting evolution including the most recent events. These basins are dammed downslope by the Eolian Islands arc system. A typical Messinian evaporitic sequence is found in these basins, but is confined to restricted depressions such as the western Cefalu Basin area (Fig. 23B). Chaotic intervals within the otherwise

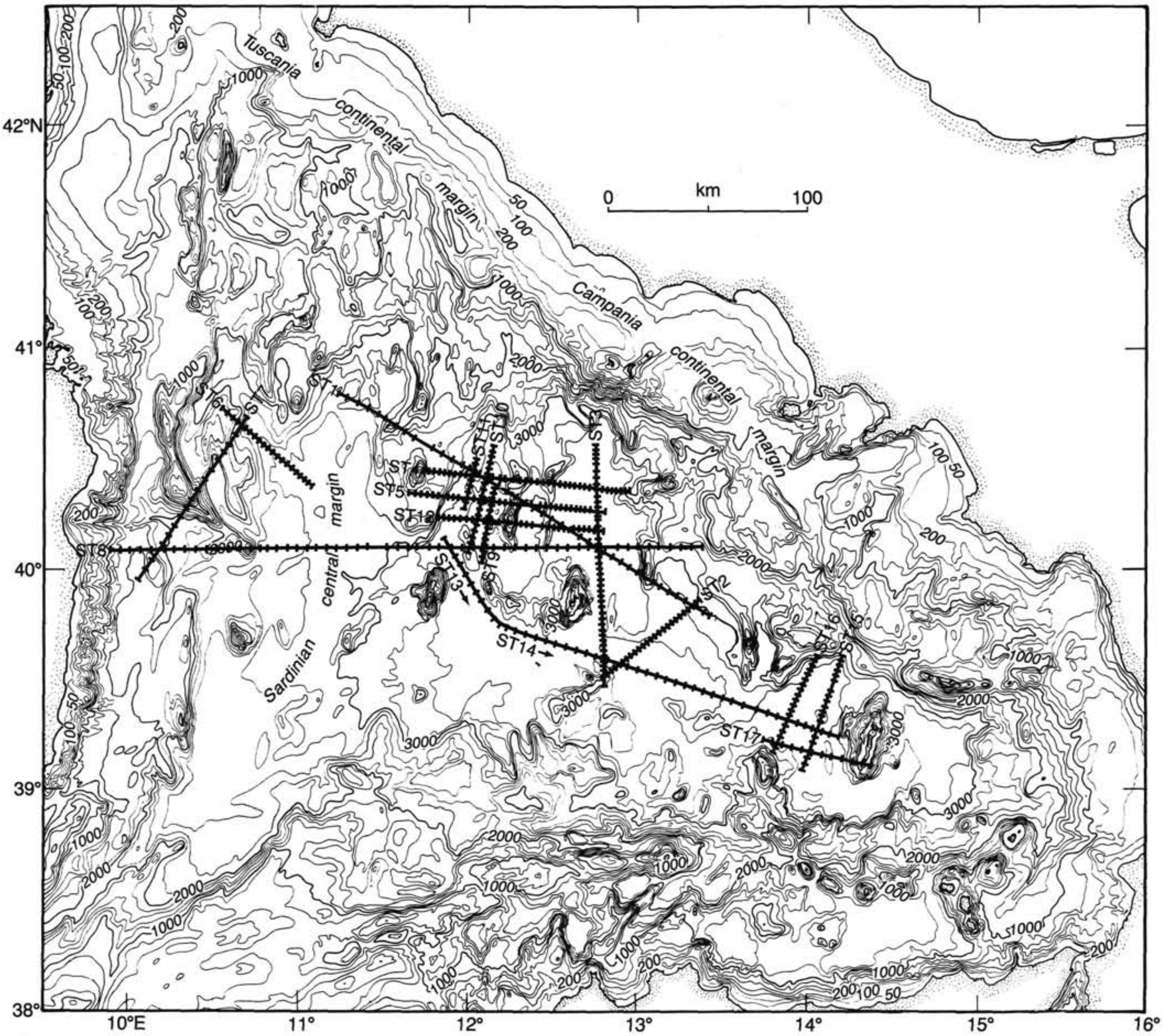


Figure 10 (Continued).

layered, ponded sediments are interpreted as slumps (Fig. 23C); since these are found primarily on the flanks of the Eolian volcanoes, they are inferred to be composed of volcanogenic material. The earliest inferred volcanogenic slumps are interbedded within the inferred Pliocene section.

## The Eolian Islands Arc

The Eolian volcanic arc comprises a series of seven merging volcanoes (Fig. 1). Geochemical analysis of lavas obtained on these volcanoes show both calc-alkaline series and shoshonitic suites, and radiometric ages indicate dominant volcanic activity during Pleistocene time. The shoshonitic eruptions apparently began more recently (dates of 0.5 Ma to present) than the calc-alkaline eruptions (dates of 1.3 Ma to present) (Barberi et al., 1973, 1974, 1977; Villari, 1980; Beccaluva et al., 1981; Keller, 1982). The occurrence of apparently volcaniclastic slumps in the Pliocene section of the Cefalu Basin suggests that the initiation of volcanism may have been older than the oldest dated samples collected on the emergent portions of the islands. The temporal evolution from calc-alkaline to shoshonitic magmatism has been interpreted as a possible consequence of changes in the Benioff zone geometry and in the rate of subduction (Barberi et al., 1973; 1974; 1977; Villari, 1980; Beccaluva et al., 1981; Keller, 1982).

## The Marsili Basin

Locked between peninsular Italy and Sicily (Fig. 2) the deep and flat-floored Marsili Basin has an almost rhombohedral shape. Like the Vavilov Basin, the Marsili Basin is bisected by a huge elliptical volcano, trending approximately N15°E and standing 3000 m above the bathyal plain (Fig. 24). Dredge stations near the top of the volcano have yielded calc-alkaline rocks of very recent age (0.2 Ma; Selli et al., 1977).

Seismic lines across the Marsili Basin show numerous interbedded lava flows near the volcano flanks (Fig. 25A). Near the western rim of Marsili Basin, dipping reflectors covered by a

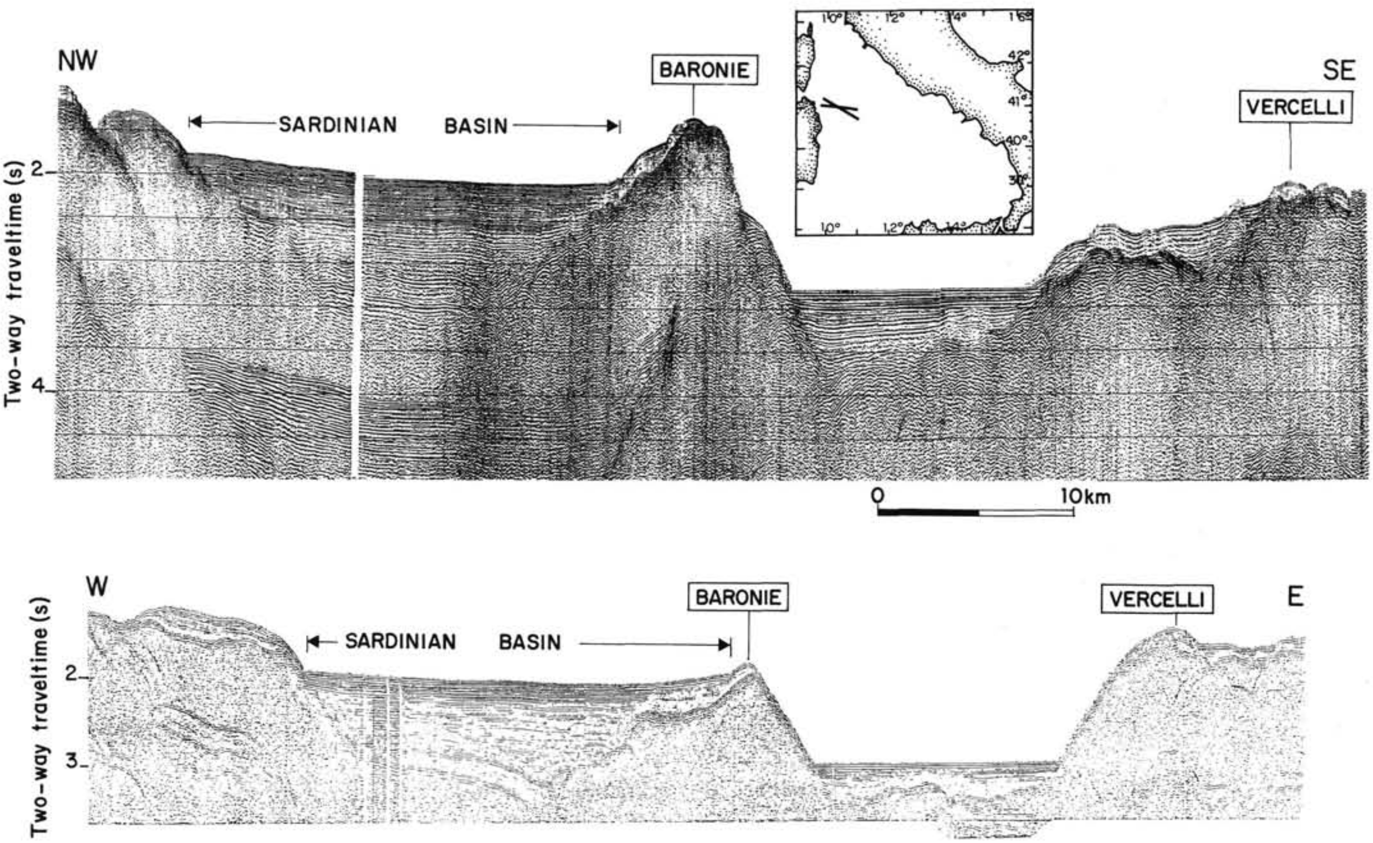


Figure 12. Two seismic lines across the Sardinia Basin and bordering Baronie and Vercelli basement highs, illustrating the seismic stratigraphy and shallow structure of the upper Sardinian margin.

thin layer of subhorizontal reflectors are interpreted as a tectonically tilted sedimentary sequence, potentially related to a recent extensional phase (Fig. 25B). Within the central part of the basin, a thick sequence of well-layered reflectors rests directly upon an irregular acoustic basement. On one recent MCS line (Fig. 25C), discontinuous reflectors can be discerned beneath this previously defined "acoustic basement" suggesting the occurrence of interbedded lava flows and sediments.

The age of the Marsili Basin sedimentary cover was inferred to be younger than the basal sediments of the Vavilov Basin. Proposed ages ranged from Messinian to lower Pliocene (Fabbri and Curzi, 1979). However, the distribution of the igneous basement within the Marsili Basin remains speculative due to the inferred presence of widespread volcaniclastics.

## THE TYRRHENIAN BASIN: SEDIMENTARY DISTRIBUTION AND STRUCTURE

The dense grid of seismic reflection surveys available for the Tyrrhenian Sea (Fig. 10) allows the construction of a set of maps covering the distribution and thickness of the pre-Messinian series, the Messinian facies distribution, the Pliocene-Pleistocene thickness, and the main structural lineaments.

The map of the distribution of the presumed pre-Messinian facies (Moussat et al., 1984; Rehault et al., 1987) illustrates the presence of relatively thick deposits on both the Sardinian and Calabrian upper margin where two distinct sedimentary cycles have often been distinguished (Fabbri et al., 1979; Moussat et al., 1984; Rehault et al., 1987). In the central basin, pre-Messinian sediments are either absent or below the resolution of the seismic records. This observation has been interpreted to suggest that the central basin had not been created at this time.

The various maps of distribution of the Messinian facies based on acoustic characters show that by late Miocene the Sardinian margin was already a subsiding basin in which thick evaporites were deposited (Fabbri and Curzi, 1979; Malinverno et al., 1981; Moussat, 1983; Rehault et al., 1987). A "marginal type evaporitic facies" has been defined (Fabbri and Curzi, 1979) based on the juxtaposition of thinly laminated strata with diffractive, apparently erosional surfaces; this facies is observed both east and west of the central basin and covers a larger area than the pre-Messinian facies. The Messinian facies of the Vavilov and Marsili Basins was mapped as volcaniclastic (Moussat, 1983) or subaerial and lacustrine (Malinverno et al., 1981).

Maps of the Pliocene-Pleistocene sedimentary thickness on Figures 20 and 26 illustrate drastic changes in the depocenters' locations relative to the pre-Messinian or Messinian. During this time interval, the Perityrrhenian slope basins still represented important sedimentary traps, but both the Vavilov and Marsili Basins acted as new large-scale depocenters. These new depocenters are elongate and oriented N10°E (Fig. 27).

Finally the mapping of the main structural trends (Fig. 26) and the structural sketch (Fig. 27) clearly demonstrates the in-

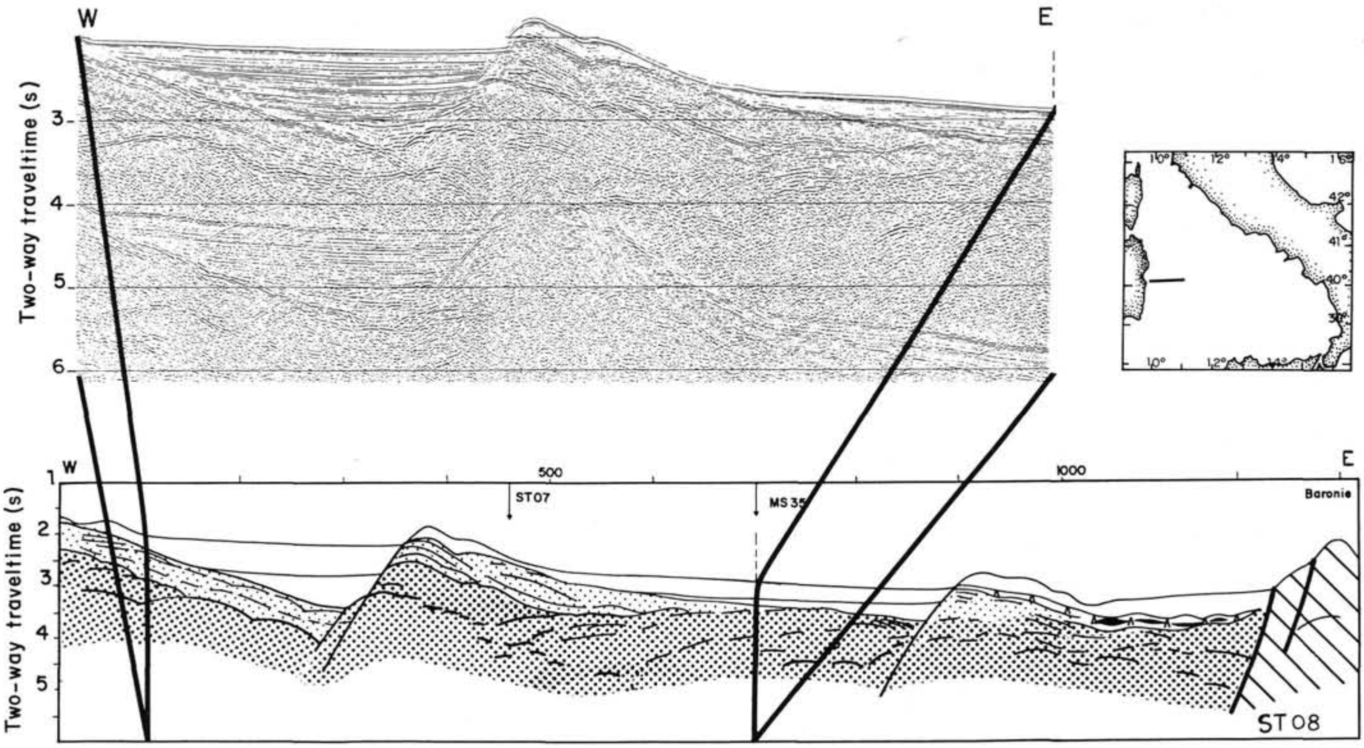


Figure 13. Multichannel seismic line ST08 (see location on Fig. 10B) illustrating the block faulting and tilting of the upper Sardinian margin. Note that the block (including pre-Messinian series and unconformities) is tilted toward the central deep basin, i.e., in a reverse position from the main distensive structures of Sardinian margin.

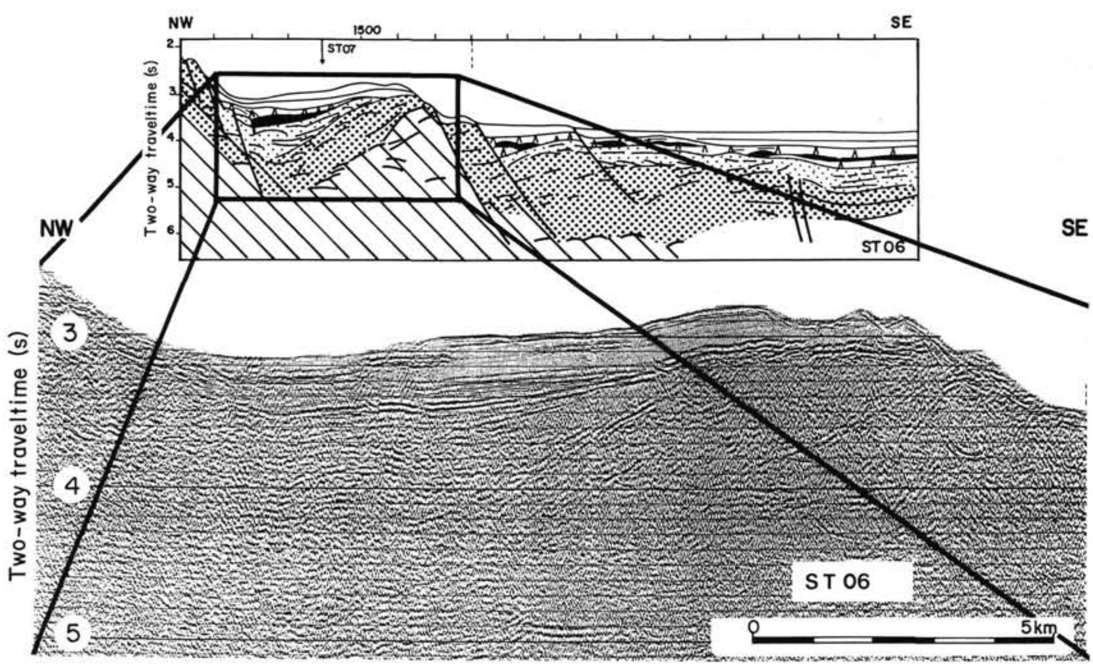


Figure 14. Multichannel seismic line ST06 across a small tilted block at the base of the Monte Baronie structure (see location on Fig. 10B). ODP Site 654 is located on this line (see "Site 654" chapter, this volume).

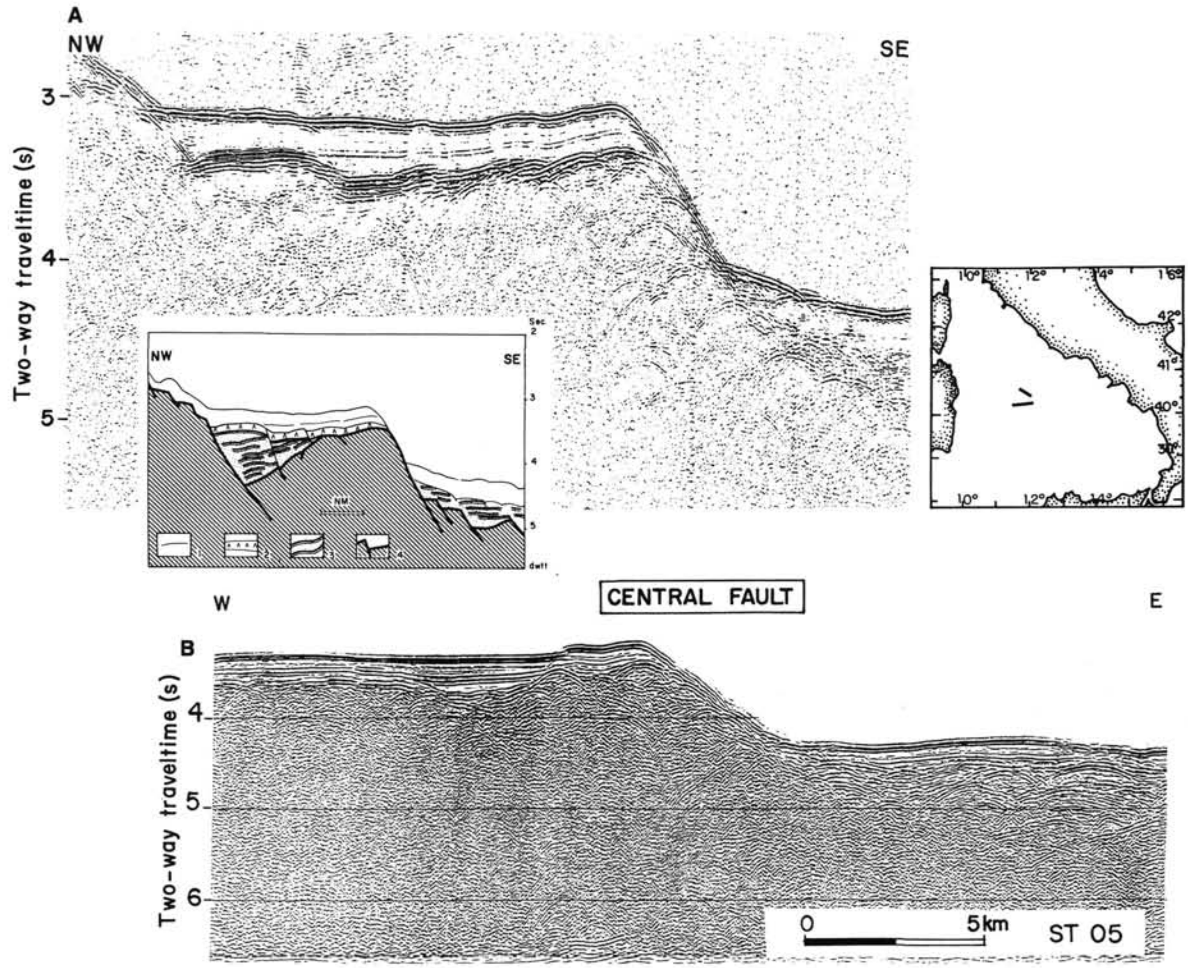


Figure 15. Two seismic lines across the Central Fault (R. Selli lineament) at the boundary between the Cornaglia Basin and the lower Sardinian margin. A. Sparker line (IGM *Bologna*) showing the detailed seismic stratigraphy including the Miocene sequences (uppermost Messinian). B. Multichannel line ST05 showing the pre-Messinian highly dislocated sequences and eroded tilted basement. Note that on this seismic section the Central Fault appears made of a series of small-amplitude fault scarps.

tense surficial fracturing of the central Tyrrhenian Basin. In this area, two dominant structural directions can be observed; north to N30°E lineaments and fractures (such as the Central Fault) are interpreted as tensional directions delineating horsts, grabens, and tilted block structures. More subtle, N100°-130°E trends are interpreted as transfer faults. These faults offset the previous faults and lie parallel to the direction of inferred Tyrrhenian Sea overall opening, that is southeastward, toward the subduction zone.

## THE TYRRHENIAN SEA: A BRIEF REVIEW OF GEODYNAMIC MODELS

The Tyrrhenian Sea has been variously interpreted as a relict of the Tethys Ocean, as a foundered continental area, as a back-arc basin, and numerous variations or combinations of these models.

In light of DSDP Site 373 results it is now unlikely (Hsü, Montadert et al., 1978) that the Tyrrhenian Sea constitutes a remnant of a Tethyan ocean.

Argand (1924) first interpreted the Tyrrhenian Sea as one of the deep Neogene basins created by drifting during the progressive shortening between Europe and Africa.

The different geodynamic models will be discussed in two categories: the models which emphasize vertical tectonics, and the models which stress horizontal motion, including models which take into account the back-arc type evolution.

### The Tyrrhenian Sea as a Consequence of Prevailing Vertical Tectonics

Following the hypothesis of Forsyth Major (1883), Selli (1970) and Selli and Fabbri (1971) consider the Tyrrhenian as resulting from a sudden and drastic continental foundering occurring during middle Pliocene time. This was a consequence of "subcrustal erosion mechanisms" and subsequent volcanism (Van Bemmelen, 1969; 1972). Morelli (1970) and Heezen et al. (1971) also interpreted the Tyrrhenian as a piece of foundered continental crust intruded by oceanic-type magmatism (Del Monte, 1972). Later on, and taking into account additional field and marine data, Selli (1981, 1985) developed a modified foundering model, still occurring in middle Pliocene time, and based on isostatic compensation resulting from oceanization. A small amount of drifting associated with arc collision phenomenon was also considered.

Wezel (1981, 1985) has proposed a relationship with a large-scale mantle diapirlike upwelling which leads first to crustal doming. Such crustal doming has been attributed to mantle fluid uprising and degassing (Locardi, 1985). This doming phase is followed by rapid foundering or "krikogenesis," which

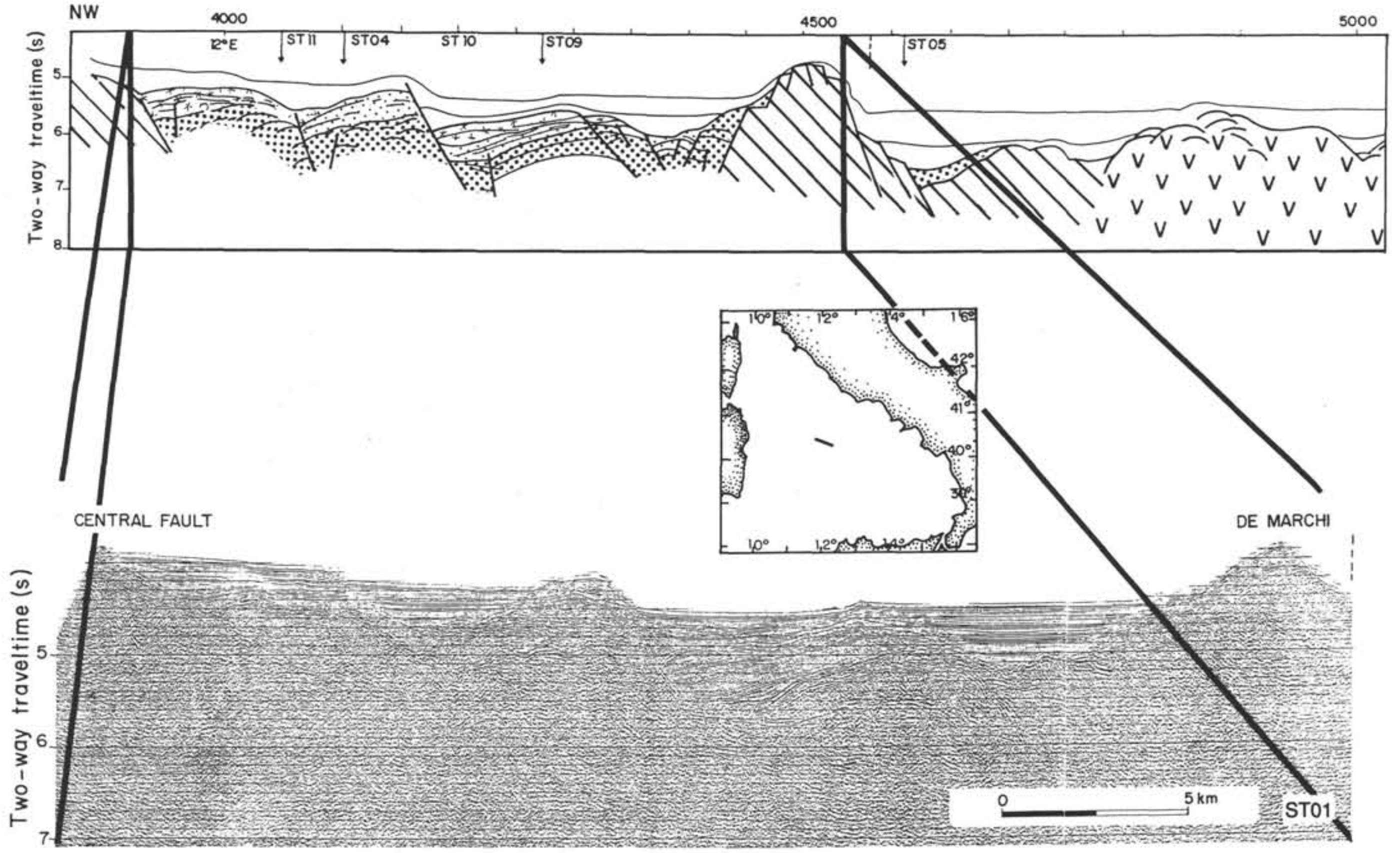


Figure 16. The lower Sardinian margin between the Central Fault (R. Selli lineament) and the deep Vavilov Basin (see location on Fig. 10B). Four main tilted blocks about 5-10 km in width develop in this area with an apparent progressive dip toward the Vavilov Basin. One, Monte de Marchi, shows the continental basement cropping out along its eastern slope. Site 652 is located on one of these tilted blocks (see "Site 652" chapter, this volume).

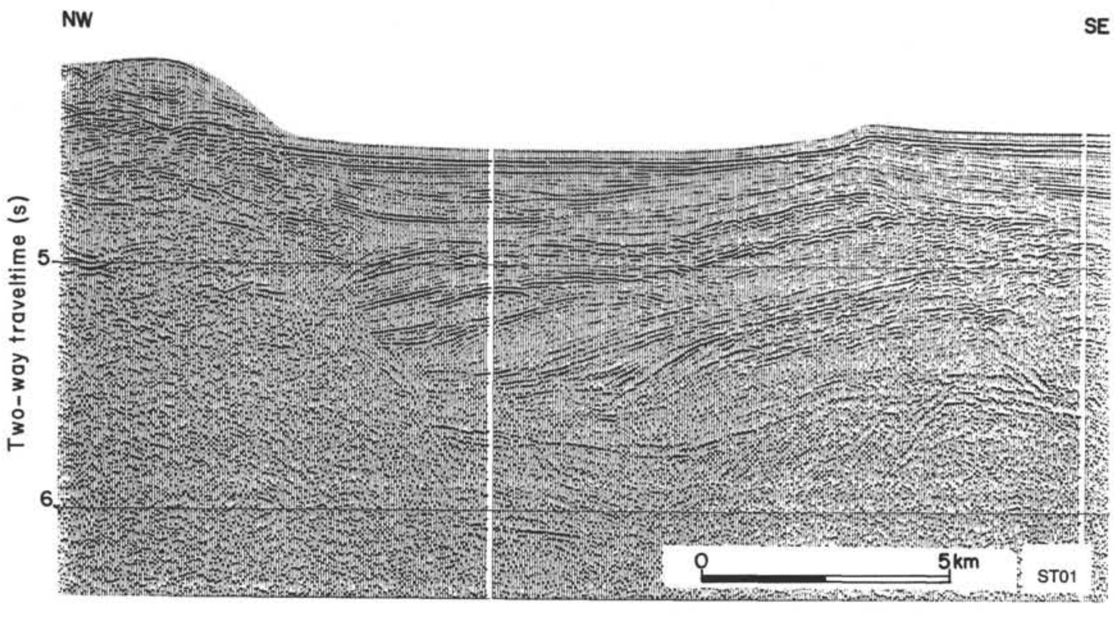


Figure 17. Detail of the processed multichannel line ST01 across one of the tilted blocks of the lower Sardinian margin. Note the prominent seismic reflector interpreted as the Miocene horizon (upper Messinian) and a thick wedge of syn-rift-shaped seismic sequence interpreted as probable Tortonian series. Site 652 is located on this tilted block.

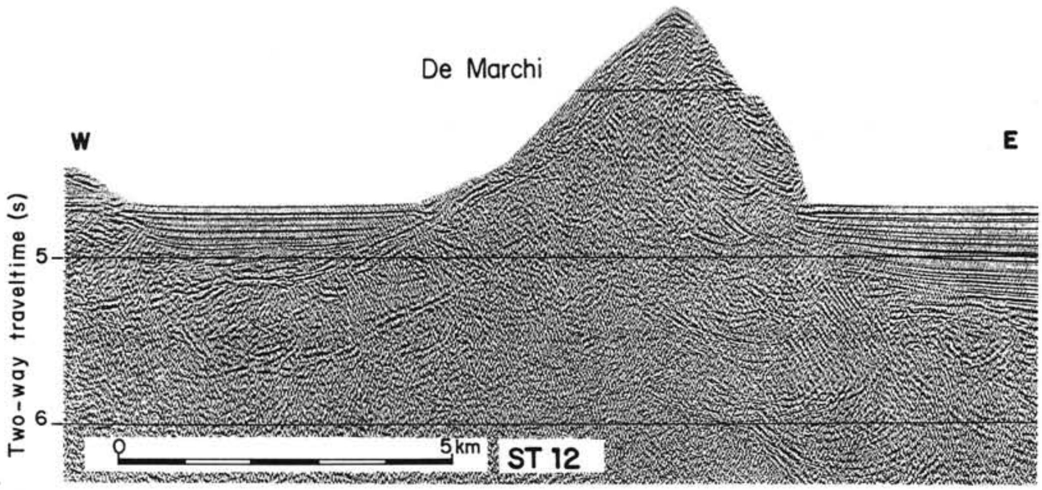


Figure 18. Processed multichannel line across Monte de Marchi, the easternmost tilted block occurring on the Sardinian margin and facing the inferred transition zone with the "oceanic-type crust." Note the strong block asymmetry and the presence of deep discontinuous reflectors indicating that the block is probably made of sedimentary strata in a pre-rift arrangement.

has been compared to a megacaldera evolution. Evidence for this evolutionary model is found in the observation of "concentric distribution of outer-arc sedimentary troughs."

## The Tyrrhenian Sea as a Consequence of Prevailing Horizontal Motions and as a Back-arc Basin

Boccaletti and Guazzone (1972) first proposed a relationship between the Tyrrhenian Sea and Apennine evolution considering the area as a marginal type basin. At the same time Alvarez et al. (1974) postulated an evolution of the Tyrrhenian governed by microplate dispersion; their evidence was drawn from the rotation of Corsica and Sardinia (Alvarez, 1972; Westphal et al., 1973). In this model the Calabrian block moved hundreds of kilometers eastward from a previous position adjacent to Corsica and Sardinia, leaving the deep Tyrrhenian basin in its wake. Dewey et al. (1973) integrated such evolution within the framework of plate tectonics and alpine system evolution. Biju Duval et al. (1977, 1978), Rehault (1981), and Rehault et al. (1984) also integrated the Tyrrhenian evolution into the general framework of the Mediterranean Sea basins. In their hypothesis both the western Mediterranean Basin and the Tyrrhenian Sea originated as a consequence of the African-Apulian lithosphere subduction. Boccaletti et al. (1976) made a comparison between the Tyrrhenian and the Panonian Basins in which they stress the main geophysical characters of the area considered as an example of back-arc basin processes.

More recently, following the hypotheses of Carey (1958) and Scandone (1979), Boccaletti et al. (1984) developed an evolutionary model of the area in which an east-west directed opening prevails. Their model, partly based on the occurrence of east-trending strike slip motion in northern Sicily, implies an eastward motion of Calabria.

Concurrently, Moussat (1983), Moussat et al. (1984), Malinverno and Ryan (1986), and Rehault et al. (1984, 1987) stress a prevailing southeastward direction of opening. In these models the evolution of the Tyrrhenian Sea is partly controlled by the locking effect of both the Apennines and Sicilids collision. The only possibility of extension remains toward the southeast, i.e., toward the present Calabrian subduction zone.

Moussat (1983) based his model mostly on microtectonic analysis and derived strike slip motion measured on shore implying a southeastward (N120°E) drift of Calabria. This model also implies a progressive sinking and subsequent "spoon" deformation of the downgoing Ionian slab as proposed by Gasparini et al. (1982).

This leads to a close relationship between the main compressional events occurring along the outer-arc system and the main extensional phases within the back-arc basin itself. In this view, the Tyrrhenian Basin can be regarded as a specific land-locked back-arc basin.

### ACKNOWLEDGMENTS

We thank particularly Dr. Kim Kastens and Christian Auroux and most of the Leg 107 scientific party for critical review of this paper, Mrs. Patricia M. Wunneburger for typing, and Yves Descatoire for most of the drafting.

### REFERENCES

AGIP, 1981. Italia: Carta Magnetica: Anomalie del Campo Magnetico Residuo, (scale 1:500,000). *Atti. Min., Direz, Espl. Idrocarburi, Met. Appl., Geofis.*, San Donato, Milano.

Alvarez, W., 1972. Rotation of the Corsica-Sardinia microplate. *Nature*, 235:103–105.

Alvarez, W., Cocozza, T., and Wezel, F. C., 1974. Fragmentation of the Alpine orogenic belt by microplate dispersal. *Nature*, 248:309–314.

Argand, E., 1924. La tectonique de l'Asie. *C.R. Int. Geol. Congr.* (13th meeting), Bruxelles, 1:171–372.

Barberi, F., Gasparini, P., Innocenti, F., and Villari, L., 1973. Volcanism of the southern Tyrrhenian Sea and its geodynamic implications. *J. Geophys. Res.*, 23:5221–5232.

Barberi, F., Innocenti, F., Ferrara, G., Keller, J., and Villari, L., 1974. Evolution of eolian arc volcanism (southern Tyrrhenian Sea). *Earth Planet. Sci. Lett.*, 21:269–276.

Barberi, F., Bizouard, H., Capaldi, G., Ferrara, G., Gasparini, P., Innocenti, F., Joron, J. L., Lambret, B., Treuil, M., and Allegre, C., 1978. Age and nature of basalts from the Tyrrhenian abyssal plain. *In* Hsü, K. J., Montadert, L., et al., *Init. Reps. DSDP*, 42 Pt. 1: (U.S. Govt. Printing Office) 509–514.

Barone, A., Fabbri, A., Rossi, S., and Sartori, R., 1982. Geological structure and evolution of the marine areas adjacent to Calabrian arc. *Earth Evol. Sci.* 3:207–221.

Bayer, M., 1977. Etude gravimetrique de la Corse [Thesis]. Univ. de Montpellier.

Beccaluva, L., Gabbianelli, G., Lucchini, F., Rossi, P. L., Savelli, C., and Zeda, O., 1981. Magmatic character and K/Ar ages of volcanics dredged from the eolian seamounts (Tyrrhenian Sea). *In* Wezel, F.C. (Ed.), *Sedimentary Basins of Mediterranean Margins.* Bologna (Tecnoprint), 361–168.

Beccaluva, L., Gabbianelli, G., Lucchini, F., Rossi, P. L., and Savelli, C., 1985. Petrology and K/Ar ages of volcanics dredged from the Eolian seamounts: implications for geodynamic evolution of the southern Tyrrhenian basin. *Earth Planet. Sci. Lett.* 74:187–208.

Biju-Duval, B., Dercourt, J., and Le Pichon, X., 1977. From the Tethys Ocean to the Mediterranean Sea. *In* Biju-Duval, B., and Montadert, L. (Eds.), *Structural History of the Mediterranean Basin*: Split, Yugoslavia (Tecnoprint), 143–164.

Biju-Duval, B., Letouzey, J., and Montadert, L., 1978. Structure and evolution of the Mediterranean basins. *Init. Repts. DSDP*, 42 (Pt. 1): Washington (U.S. Govt. Printing Office), 951–984.

Boccaletti, M., and Guazzone, G., 1972. Gli archi apennici, il Mar Ligure ed il Mar Tirreno nel quadro della tettonica dei bacini marginali retro-arco. *Mem. Soc. Geol. Ital.*, 11,2:201–216.

Boccaletti, M., and Manetti, P., 1978. The Tyrrhenian Sea and adjoining regions. *In* Nairn, A.E.M., et al. (Ed.), *The Oceans Basins and Margins*: New York (Plenum), 149–191.

Boccaletti, M., Horvath, F., Loddo, M., Mongelli, F., and Stegena, L., 1976. The Tyrrhenian and Pannonian basins: a comparison of two Mediterranean interarc basins. *Tectonophysics*, 35:45–69.

Boccaletti, M., Nicolich, R., and Tortorici, L., 1984. The Calabrian Arc and the Ionian Sea in the dynamic evolution of the Central Mediterranean. *Mar. Geol.* 55:219–245.

Calcagnile, G., Mascia, U., Del Gaudio, V., and Panza, G. F., 1984 Deep structure of southeastern Europe from Rayleigh waves. *Tectonophysics*, 110,3/4:189–200.

Caputo, M., Panza, G. F., and Postpischl, D., 1972. New evidences about deep structure of the Lipari arc. *Tectonophysics*, 15,219–231.

Carey, S. W., 1958. A tectonic approach to continental drift. *Continental Drift, a Symposium,* Univ. Tasmania, 177–355.

Channel, J.E.T., 1986. Paleomagnetism and continental collision in the Alpine Belt and the formation of late-tectonic extensional basins. *In* Coward, M. P., and Ries, A. C. (Eds.), *Geol. Soc. London, Spec. Publ.* 19:261–286.

Channel, J.E.T., D'Argenio, B., and Horvath, F., 1979. Adria, the African promontory, in Mesozoic Mediterranean paleogeography. *Earth Sci. Rev.*, 15:213–292.

Colantoni, P., Fabbri, A., Gallignagni, P., Sartori, R., and Rehault, J. P., 1981. Carta litologica e stratigrafica dei mari italiani. Firenze (Litografica Artistica Cartografica).

Colombi, B., Gieze, P., Luongo, G., Morelli, C., Riuscetti, M., Scarascia, S., Schutte, K. G., Stowald, J., and De Visentini, G., 1973. Preliminary report on the seismic refraction profile Gargano-Salerno-Pantellaria. *Boll. Geofis. Teor. Appl.*, 15,59:225–254.

Curzi, P., Fabbri, A., and Nanni, T., 1980. The Messinian evaporitic event in the Sardinian basin area (Tyrrhenian Sea). *Mar. Geol.* 34, 53/54:157–170.

Dal Piaz, G. V., Del Moro, A., Sabatino, B., Sartori, R., and Savelli, C., 1983. Geologia del Monte Flavio Gioia (Tirreno centrale). *Mem. Sci. Geol.* Univ. Padova, 35:429–452.

Del Monte, M., 1972. Il vulcanesimo del Mar Tirreno: Nota priliminare sui volcani Marsili e Palimoro. *G. Geol.* 38:231–252.

Della Vedova, B., Pellis, G., Foucher, J. P., and Rehault, J. P., 1984. Geothermal structure of the Tyrrhenian Sea. *Mar. Geol.*, 55:271–289.

Dewey, J. F., Pitmann, W. C., Ryan, W.B.F., and Bonnin, J., 1973. Plate tectonics and the evolution of the Alpine system. *Geol. Soc. Am. Bull.*, 84:3137–3180.

Dietrich, V., Emmermann, R., Puchlt, H., and Keller, J., 1978. Oceanic basalts from the Tyrrhenian Basin, DSDP Leg 42A, Hole 373A. *In* Hsü, K. J., Montadert, L., et al., (Eds.), *Init. Repts. DSDP*, 42, Pt. 1: Washington (U.S. Govt. Printing Office), 515–530.

Duschenes J., Sinha, M. C., and Louden, K. E., 1986. A seismic refraction experiment in the Tyrrhenian Sea. *Geophys. J. R. Astron. Soc.* 85:139–160.

Erickson, A. T., 1970. Heat flow measurements in the Mediterranean, Black and Red seas [Thesis]. Mass. Inst. Technol.

Erickson, A. J., and Von Herzen, R., 1978. Downhole temperature measurements. Deep Sea Drilling Project, Leg 42A. *In* Hsü, K. J., Montadert, L., et al. (Eds.), *Init. Repts. DSDP*, 42, Pt. 1: Washington (U.S. Govt. Printing Office), 857–871.

ESCARMED, 1982. Donnees nouvelles sur les marges du bassin ionien profond (Mediterranee orientale): resultats des campagnes Escarmed. *Rev. Inst. Fr. Petrol.*, 37,6:713–731.

Fabbri, A., and Curzi, P., 1979. The Messinian of the Tyrrhenian Sea: Seismic evidence and dynamic implications. *G. Geol.*, 43,215–248.

Fabbri, A., and Nanni, T., 1980. Seismic reflexion study of the Sardinian Basin (Tyrrhenian Sea). *Geol. Mediterr.* 7:161–178.

Fabbri, A., and Selli, R., 1972. The structure and stratigraphy of the Tyrrhenian Sea. *In* Stanley, D. J. (Ed.), The Mediterranean Sea, a natural sedimentation laboratory. Stroudsburg, PA (Dowden, Hutchinson, Ross), 75–81.

Fabbri, A., Ghisetti, F., and Vezzani, L., 1980. The Peloritani-Calabria range and the Gioia Basin in the Calabrian arc (Southern, Italy): relationships between land and marine data. *Geol. Rom.* 19:131–150.

Fabbri, A., Gallignani, P., and Zitellini, N., 1981. Geologic evolution of the peri-Tyrrhenian sedimentary basins of Mediterranean margins. *In* Wezel, F. C. (Ed.), *Sedimentary Basins of Mediterranean Margins.* Bologna (Tecnoprint), 101–126.

Finetti, I., 1982. Structural, stratigraphy and evolution of central Mediterranean. *Boll. Geofis. Teor. Appl.*, 24,96:247–312.

Finetti, I., and Morelli, C., 1973a. Geophysical exploration of the Mediterranean sea. *Boll. Geofis. Teor. Appl.,* 15,60:263–344.

________, 1973b. Wide-scale digital seismic exploration of the Mediterranean sea. *Bull. Geol. Soc. Gr.*, 10,1:65–66.

Forsyth Major, C. J., 1883. L'Origine della Fauna delle nostre isole. *Atti Soc. Tosc. Sci. Nat.*, 3:36–42,113–133,192.

Galdeano, A., and Rossignol, J. C., 1977. Assemblage a altitude constante des cartes d'anomalies magnetiques couvrant l'ensemble du bassin occidental de la Mediterranee. *Bull. Soc. Geol. Fr.*, 7,19:461–468.

Gasparini, C., Iannacone, I., Scandone, P., and Scarpa, R., 1982. Seismotectonics of the Calabrian Arc. *Tectonophysics*, 84:267–286.

Gennesseaux, M., Rehault, J. P., Thomas, B., Colantoni, P., Fabbri, A., Lepvrier, C., Mascle, G., Mauffret, A., Polino, R., Robin, C., and Vanney, J. R., 1986. Resultats des plongees en submersible Cyana sur les blocs continentaux bascules et le volcan Vavilov (mer Tyrrhenienne centrale). *C.R. Acad. Sci. Ser.* 2, 12:785–792.

Ghisetti, F. A., and Vezzani, L., 1981. Contribution of structural analysis to understanding the geodynamic evolution of the Calabrian Arc (southern Italy). *J. Struct. Geol.*, 3,4:371–381.

Heezen, B. C., Gray, C., Segre, A. G., and Zarudski, E.F.K., 1971. Evidence of foundered continental crust beneath the central Tyrrhenian Sea. *Nature*, 229:327–329.

Hsü, K. J., 1978. Tectonic evolution of the Mediterranean Basins. *In* Nairn, A.E.M., et al. (Eds.), *The Ocean Basins and Margins.* New York (Plenum), 29–76.

Hsü, K. J., Montadert, L., et al., 1978. Site 373: Tyrrhenian Basin. *Init. Repts. DSDP*, 42 Pt. 1: Washington (U.S. Govt. Printing Office), 151–174.

Hutchinson, I., Von Herzen, R. P., Louden, K., Sclater, J. G., and Jemseck, J. P., 1985. Heat flow in the Balearic and Tyrrhenian Basins, Western Mediterranean. *J. Geophys. Res.*, 90,B1:685–701.

Keller, J., 1982. Mediterranean island arcs. *In* Thorpe, R. S. (Ed.): *Andesites.* Wiley (Chichester), 307-325.

Locardi, E., 1985. Neogene and Quaternary Mediterranean volcanism: the Tyrrhenian example. *In* Stanley, D. J. and Wezel, F. C. (Eds.), *Geological Evolution of the Mediterranean Basin.* New York (Springer), 273–291.

Lort, J. M., 1977. Geophysics of the Mediterranean Sea basins. *In* Nairn, A.E.M., Kanes, W. H., and Stehli, G. (Eds.), *The Ocean Basins and Margins,* New York (Plenum), 151–213.

Malinverno, A., and Ryan, W.B.F., 1986. Extension in the Tyrrhenian sea and shortening in the Apennines as result of arc migration driven by sinking of the lithosphere. *Tectonics*, 5,2:227–245.

Malinverno, A., Cafiero, M., Ryan, W.B.F., and Cita, M. B., 1981. Distribution of Messinian sediments and erosional surfaces beneath the Tyrrhenian Sea: Geodynamic implications. *Oceanol. Acta.*, 4: 489–496.

Morelli, C.,1970. Physiography, gravity and magnetism of the Tyrrhenian Sea. *Boll. Geofis. Teor. Appl.*, 12,48:275–309.

________, 1975. The gravity map of Italy. *In* Ogniben, L., Parotto, M., and Praturlon, A. (Eds.), *Structural Model of Italy.* Quad. Ric. Sci. 427–448.

Morelli, C., Giese, P., Cassinis, R., Colombi, B., Guerra, I., Luongo, G., Scarascia, S., and Schutte, K. G., 1975a. Crustal structure of southern Italy; a seismic refraction profile between Puglia-Calabria-Sicily. *Boll. Geofis. Teor. Appl.*, 17:183–210.

Morelli, C., Pisani, M., and Gantar, G., 1975b. Geophysical anomalies and tectonics in the Western Mediterranean. *Boll. Geof. Teor. Appl.*, 17:67.

Moussat, E., 1983. Evolution de la Mer Tyrrhenienne centrale et orientale et de ses marges septentrionales en relation avec la neotectonique dans l'arc calabrais [Thesis]. Univ. Pierre et Marie Curie, Paris.

Moussat, E., Rehault, J. P., Fabbri, A., and Mascle, G., 1985. Evolution geologique de la Mer Tyrrhenienne. *C.R. Acad. Sci. Ser.* 2,7: 491-496.

Moussat, E., Rehault, J. P., and Fabbri, A., 1986. Rifting et evolution tectonosedimentaire du Bassin Tyrrhenien au cours du Neogene et du Quaternaire. *G. Geol.* (spec. issue).

Nicolich, R., 1981. Il profilo Latina-pescara e le registrazione mediante Obs nell Mar Terreno. *Naz. Geofis. Terra Solida*, (1st meeting) Rome. 3-5 Nov 1981.

Panza, G. F., Calcagnile, G., Scandone, P., and Mueller, S., 1980. La struttura profonda dell'area mediterranea. *Scienze*, 141:60-69.

Recq, M., Rehault, J. P., Steinmetz, L., and Fabbri, A., 1984. Amincissement de la croute et accretion au centre du Bassin Tyrrhenien d'apres la sismique refraction. *Mar. Geol.* 55:411-428.

Rehault, J. P., 1981. Evolution tectonique et sedimentaire du Bassin Ligure (Mediterranee occidentale) [Thesis]. Univ. Pierre et Marie Curie, Paris.

________, 1985. Geologie des bassins Ligure et Tyrrhenien. *Assn. Ital. Oceanol. Limnol.* (6th Cong.) Livorno, 23-48.

Rehault, J. P., Boillot, G., and Mauffret, A., 1984. The Western Mediterranean Basin geological evolution. *Mar. Geol.*, 55:447-477.

Rehault, J. P., Mascle, J., and Boillot, G., 1984. Evolution de la Mediterranee depuis l'Oligocene. *Bull. Soc. Geol. Ital.*, 27:85-96.

Rehault, J. P., Moussat, E., and Fabbri, A., 1987. Structural evolution of the Tyrrhenian back-arc basin. *Mar. Geol.*, 74,1:123-150.

Rossi, S., and Sartori, R., 1981. A seismic reflection study of the external Calabrian arc in the northern Ionian sea (Eastern Mediterranean). *Mar. Geophys. Res.*, 4:403-426.

Ryan, W.B.F., 1973. Geodynamic implications of the Messinian crisis of salinity. *In* Drooger, C. W. (Ed.), *Messinian Events in the Mediterranean,* Amsterdam (North-Holland), 26-38.

Ryan, W.B.F., Hsü, K. J., et al., 1973. *Init. Repts. DSDP*: Washington (U.S. Govt. Printing Office), 403-464.

Scandone, P., 1979. Origin of the Tyrrhenian Sea and Calabrian Arc. *Boll. Soc. Geol. Ital.*, 98:27-34.

Schutte, K. G., 1978. Crustal structure of Southern Italy. *In* Closs, H., Roeder, D., and Schmidt, K. (Eds.), *Alps, Apennines Hellenides.* Stuttgart, 315-321.

Selli, R., 1970. Cenni morfologici generali sul Mar Tirreno. *In* Selli, R. (Ed.) *Ricerche Geologiche Preliminari nel Mar Tirreno.*, G. Geol., 37,1:5-24.

________, 1974. Appunti sulla geologia del Mar Tirreno. In Paleogeografia del Terziaro sardo nell'Ambito del Mediterraneo Occidentale. *Rend. Semin. Fac. Sc. Univ. Cagliari* Suppl., 327-351.

________, 1981. Thoughts on the geology of the Mediterranean region. *In* Wezel, F. C. (Ed.), *Sedimentary Basins of Mediterranean margins.* Bologna (Tecnoprint), 489-501.

________, 1985. Tectonic evolution of the Tyrrhenian Sea. *In* Stanley, D. J., and Wezel, F. C. (Eds.), *Geological Evolution of the Mediterranean Basin.* New York (Springer), 131-151.

Selli, R., and Fabbri, A., 1971. Tyrrhenian: a Pliocene deep-sea. *Rend. Atti Accad. Naz. Lincei.*, 50,5:580-592.

Selli, R., Lucchini, F., Rossi, P. L., Savelli, C., and del Monte, M., 1977. Dati geologici, petrochimici e radiometrici sui volcani centro-tirrenici. *G. Geol.*, 2,42:221-246.

Steinmetz, L., Ferruci, F., Hirn, A., Morelli, C., and Nicolich, R., 1983. A 550 km long Moho traverse in the Tyrrhenian sea from O.B.S. recorded Pn waves. *Geophys. Res. Lett.*,10,6:428-431.

UNESCO, 1981. *International Bathymetry Chart of the Mediterranean Intergovernmental Commission.* Paris (UNESCO).

Van Bemmelen, R. W., 1969. Origin of the Western Mediterranean Sea. *Trans. R. Geol. Mining. Soc. Neth.*, 26:13-52.

________, 1972. Driving forces of the Mediterranean orogeny (Tyrrhenian test case). *Geol. Mijnbouw.* 51:548-573.

Villari, L., 1980. The Aeolian Islands. *In* Villari, L. (Ed.), An active volcanic arc in the Mediterranean Sea. *Rend. Soc. Ital. Mineral. Petrol.*, 36,1:369-414.

Westphal, M., Barbon, C., Bossert, A., and Hamzeh, R., 1973. A computer fit of Corsica and Sardinia against southern France. *Earth Planet. Sci. Lett.*, 18:137-140.

Wezel, F. C., 1981. The structure of the Calabro-Sicilian Arc: Krikogenesis rather than subduction. *In* Wezel, F. C. (Ed.), *Sedimentary basins of Mediterranean Margins,* Bologna (Tecnoprint), 485-487.

________, 1985. Structural features and basin tectonics of the Tyrrhenian Sea. *In* Stanley, D. J. (Ed.), *Geological Evolution of the Mediterranean Basins.* New York (Springer), 153-194.

Zolotarev, V. G., and Sochel'nikov, V. V., 1980. Geothermal conditions of the African-Sicilian Rise. *Izv. Earth Phys.*, 16,3:202-206.

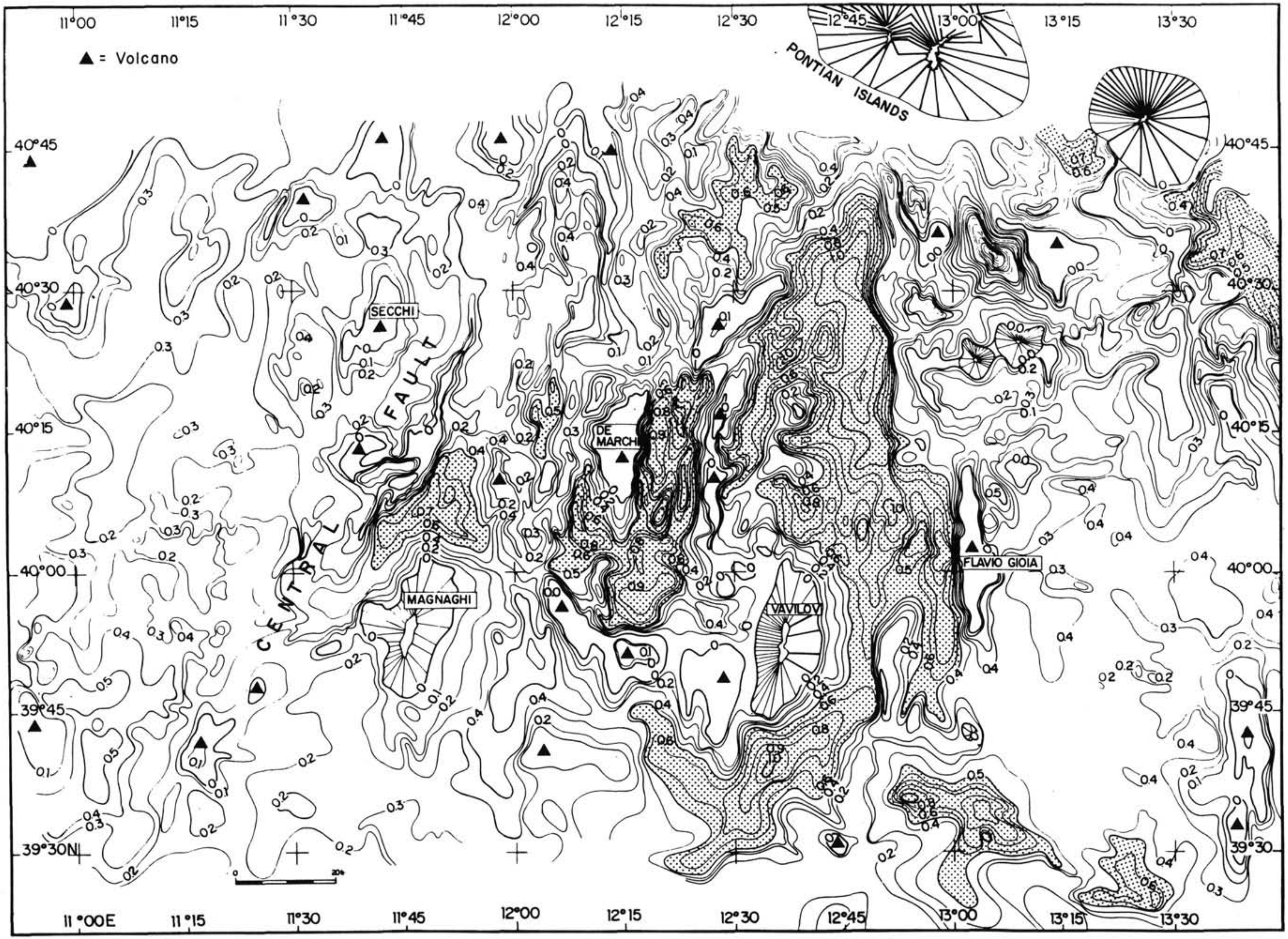


Figure 20. Isopach map of the Pleistocene-Pliocene series within the Magnaghi-Vavilov Basin and surrounding margins (after Moussat, 1983). Contour interval: 0.1 s twtt (i.e., about 100 m). The average thickness of the Pliocene-Pleistocene cover on both margins is about 250 m. Within the Vavilov Basin, thickness higher than 0.5 s has been outlined by dotted lines. The Vavilov Seamounts are elongated northward through a series of disconnected basement swells bisecting the entire basin.

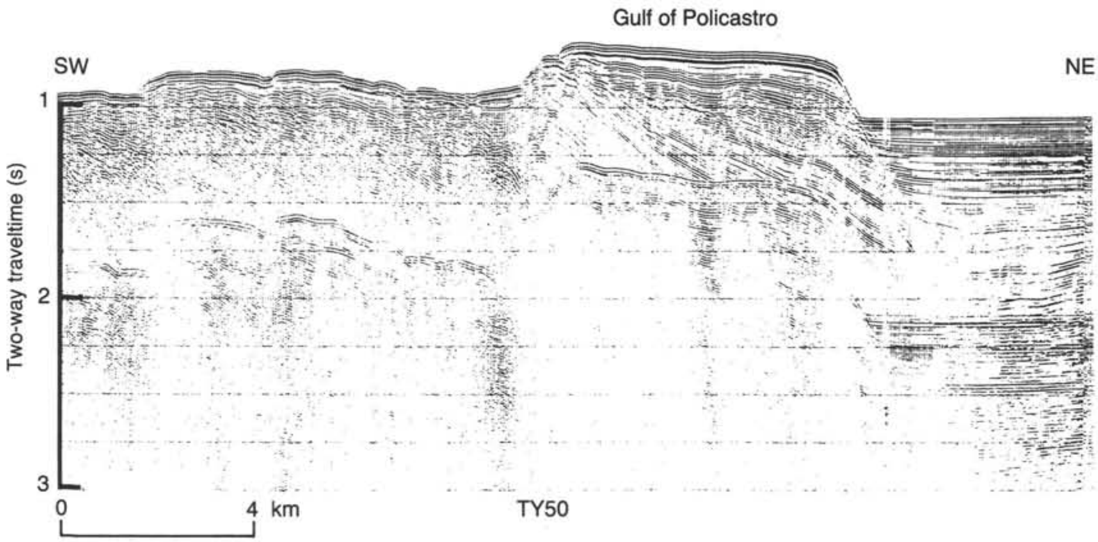


Figure 21. Example of a recent active tensional tectonic feature occurring on the upper Apenninic margin within the Gulf of Policastro. This tensional tectonic feature has been related to a general transcurrent motion occurring along the eastern Tyrrhenian margin.

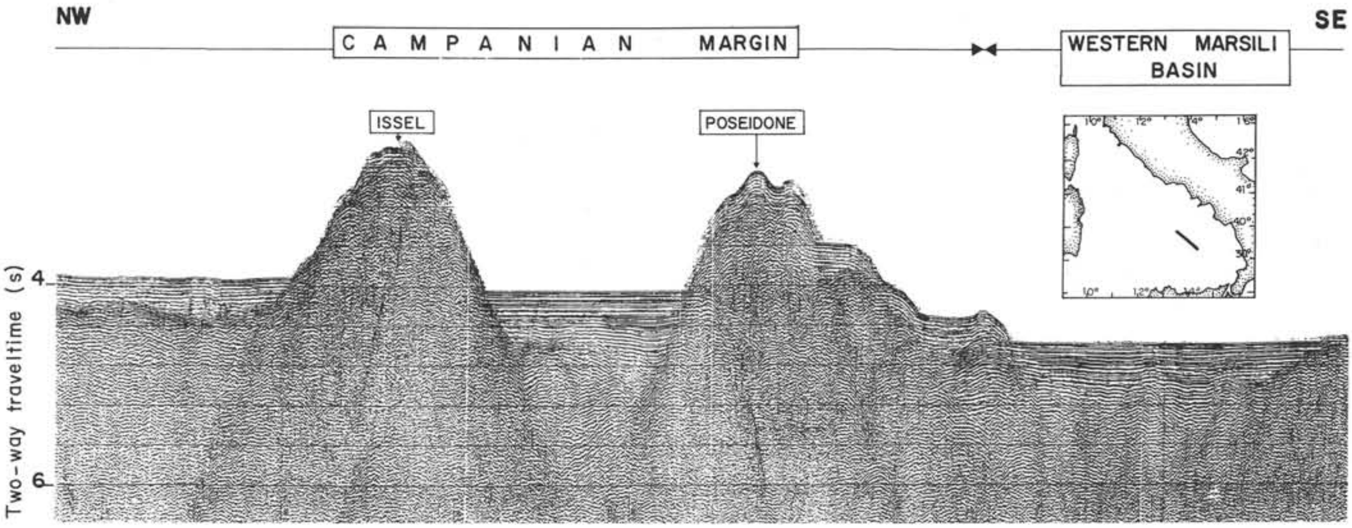


Figure 22. A seismic section across the Campanian margin area and between Vavilov (northwest) and Marsili (southeast) basins. The margin is cut by large-scale distensive blocks (Monte Issel and Poseidone, respectively). Each of these blocks appears slightly tilted toward Vavilov Basin (Issel) and Marsili Basin (Poseidone).

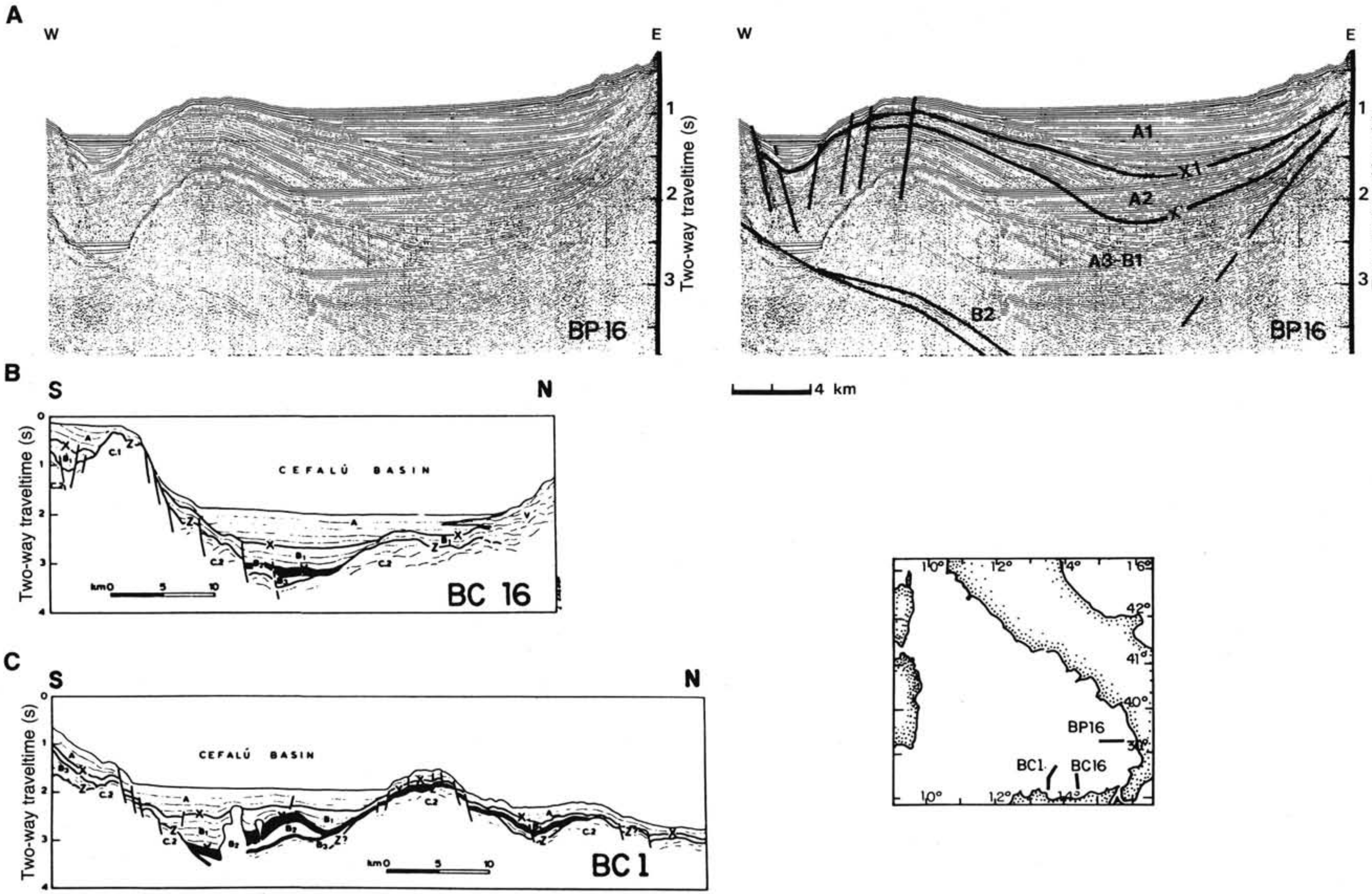


Figure 23. Seismic sections across the Perityrrhenian basins off Calabria and Sicily. A. Interpreted sparker line across Paola Basin showing a thick asymmetric basin bounded eastward by a large-scale normal fault system. Note that the inferred uppermost Miocene is highly dislocated and outlines the top of a large-scale tilted block. B. Interpreted sparker lines across Cefalu Basin (after Fabbri et al., 1981). Symbols A and B1, B2, and B3 indicate the Pleistocene-upper Pliocene, the evaporite-bearing Messinian, and the presumed Tortonian, respectively. C. Symbols C2, X, and Z refer to pre-Tortonian formation and to two main unconformities observed within the Perityrrhenian basins, respectively. Symbol V indicates interbedded volcaniclastics and lava flows.

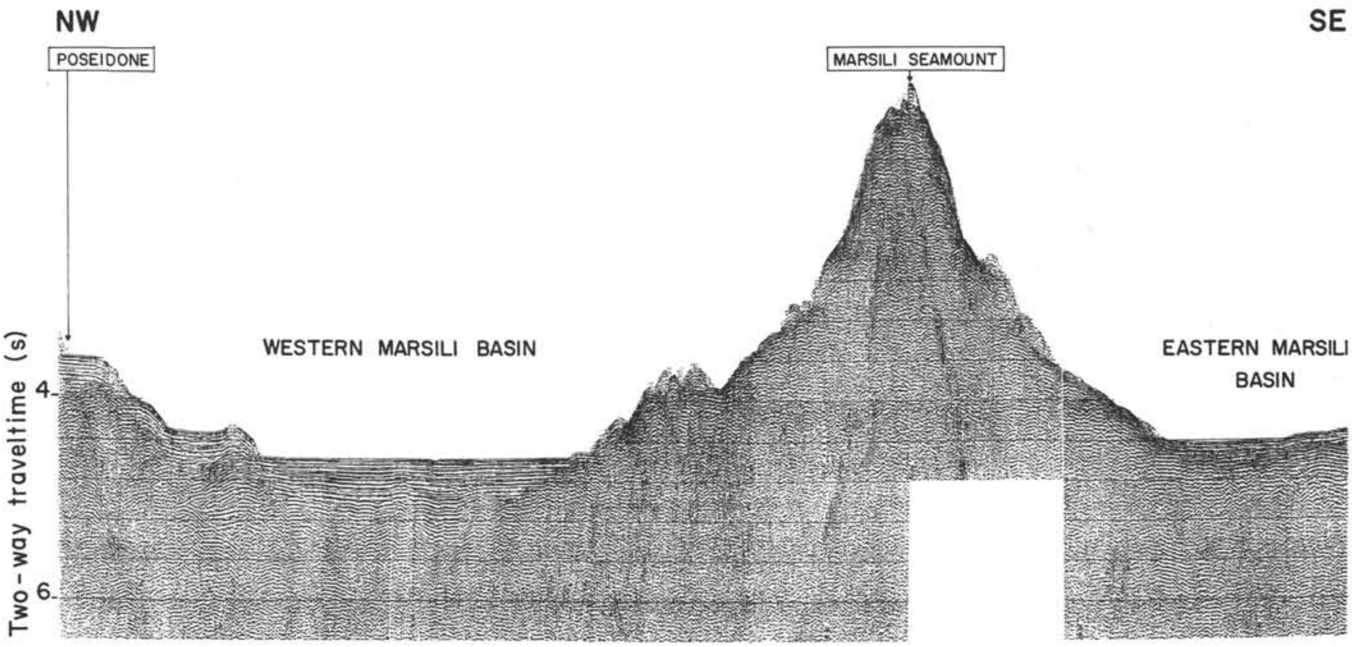


Figure 24. A seismic line across the Marsili Basin and Marsili Seamount. The seamount constitutes a sedimentary dam for Calabria- and Sicily-derived sedimentary supply.

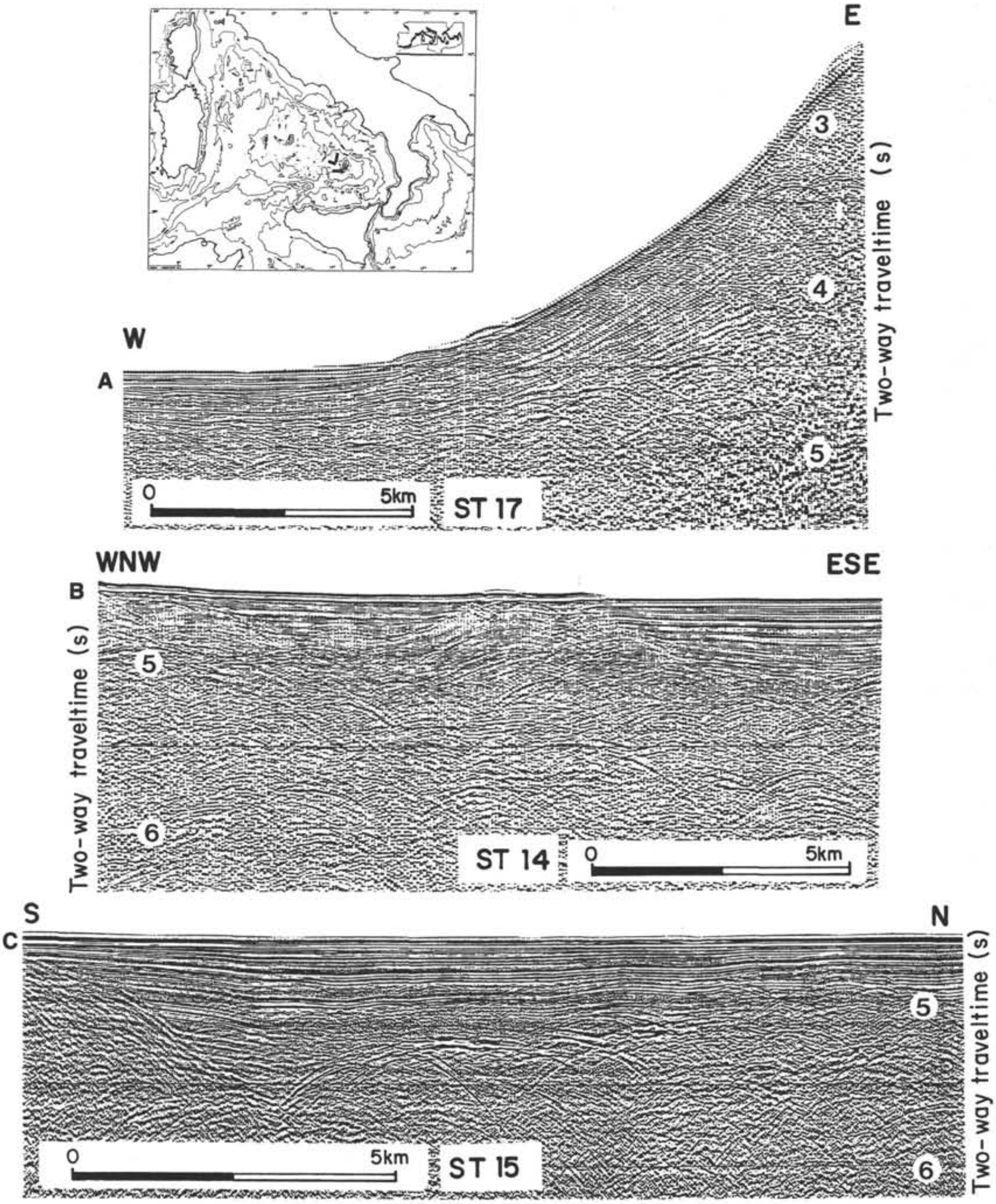


Figure 25. Three sections of multichannel seismic lines across the Marsili Basin area. A. Western flank of the Marsili Seamount showing interbedded lava flows within the basin filling. B. Example of recent deformation (tilting) occurring at the base of the Campanian margin near the transition with the Marsili Basin. C. Example of the sedimentary cover and of the basement acoustic character within the Marsili Basin. Note the presence of widespread intense seismic reflections within the sedimentary fill interpreted as large-scale turbidite sequence and volcaniclastics. Note also the rather discontinuous and weak acoustic character of the inferred igneous basement.

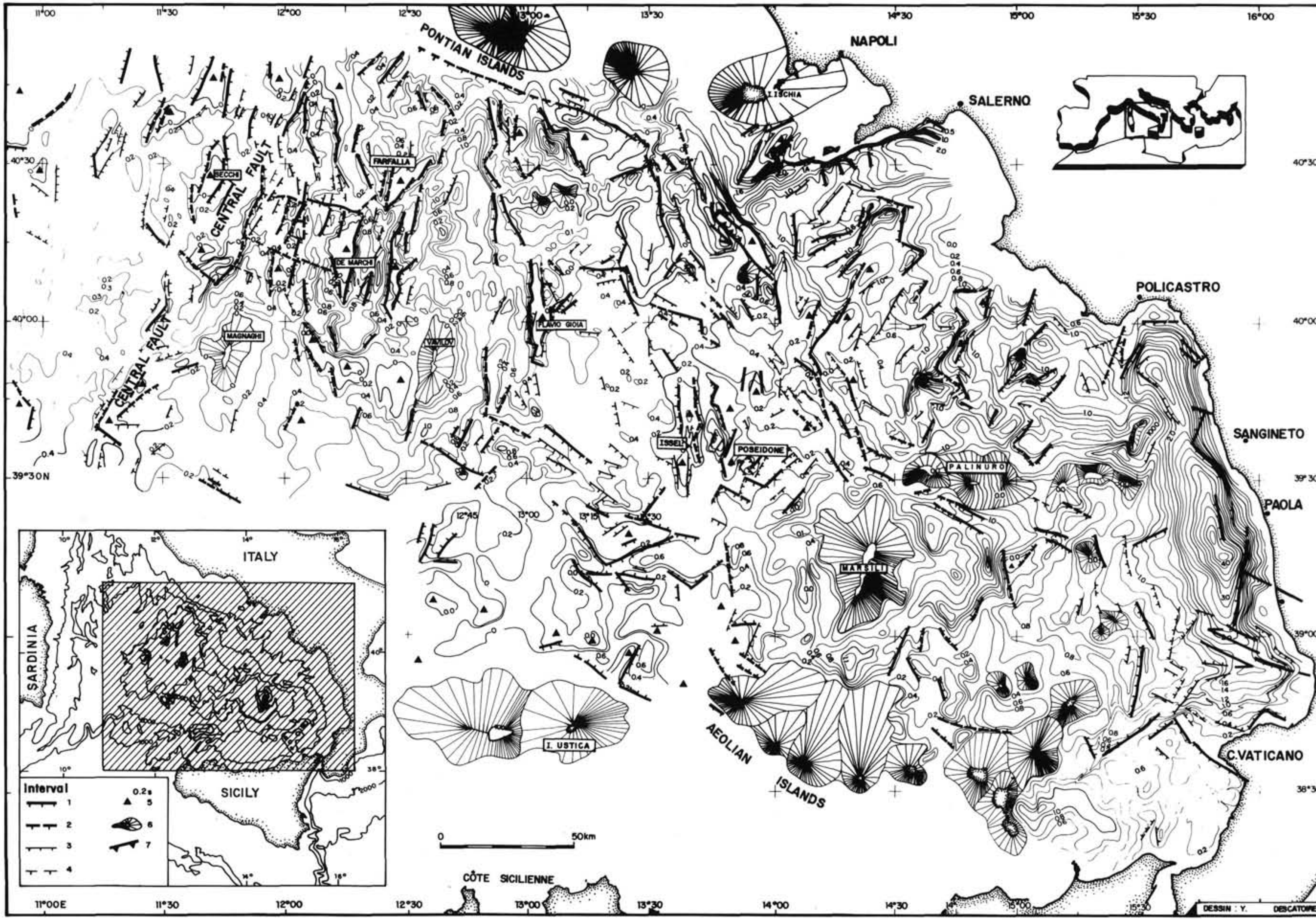


Figure 26. General Pliocene-Quaternary isopach and main tectonic features detected within the central Tyrrhenian Sea and along the Apenninic and Calabrian margin. Contour interval: 0.2 s twtt. 1. Fault scarp greater than 500 ms; 2. Inferred fault scarp greater than 500 ms; 3. Fault scarp between 200 and 500 ms; 4. Inferred fault scarp between 200 and 500 ms; 5. Nonvolcanic submarine mountain; 6. Volcano; 7. Thrust fault. After Moussat et al. (1986).

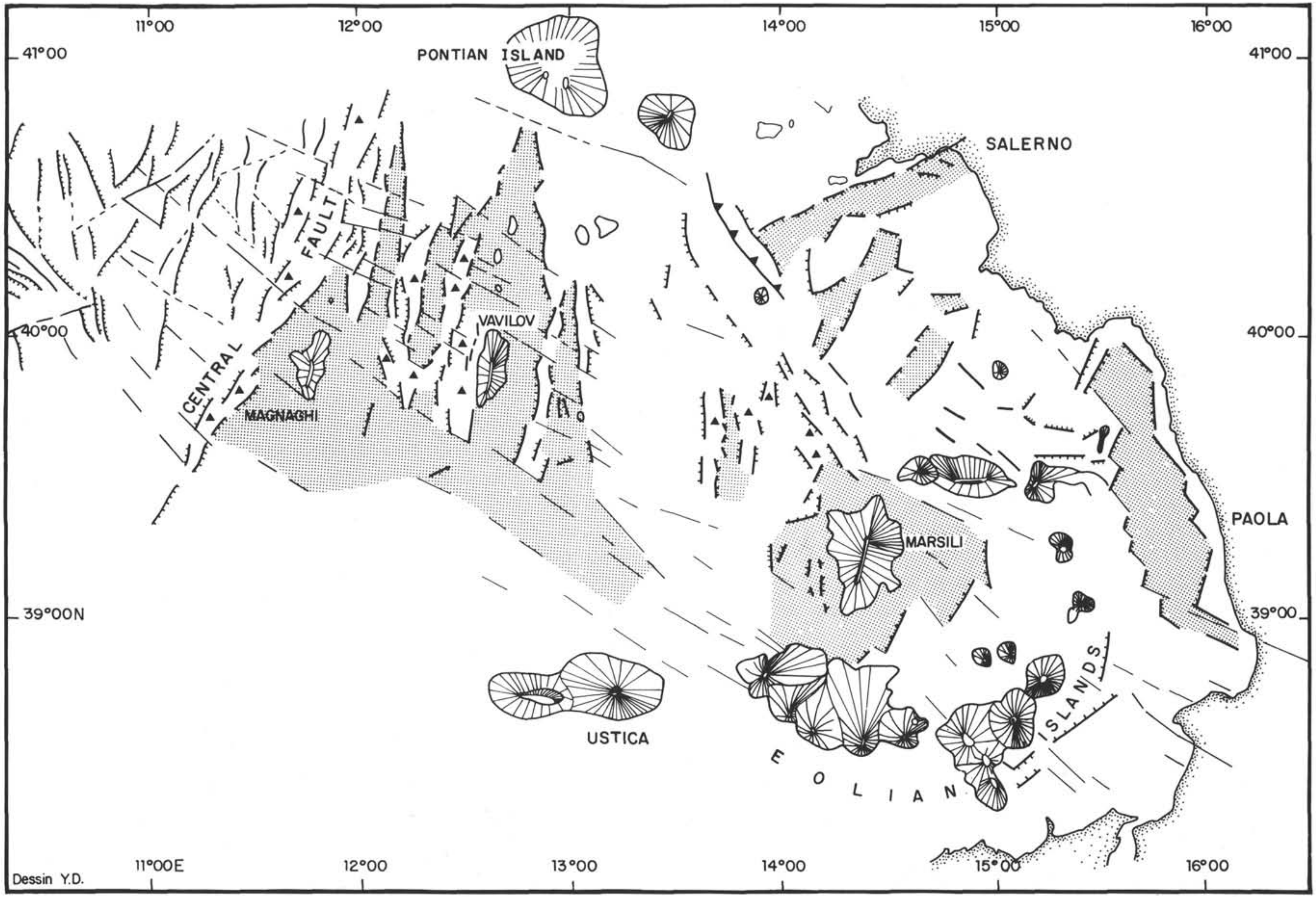


Figure 27. Highly simplified structural sketch of the present-day central Tyrrhenian Sea and surrounding margins. The main depocenters are stippled. This sketch outlines the apparent rift-type evolution of the Magnaghi-Vavilov Basin where N0°–N30°E distensive lineaments are prevailing and where N100°–N130°E more discrete lineaments are interpreted as transfer faults. The Apenninic and Calabrian margins appear structurally ruled by strike-slip motion leading to a series of complex transpressive and transtensive features and pull-apart basins. The Marsili Basin does not show any significant trend except its N20°E main elongation and rhombohedral shape. Note also the arcuate shape of the Eolian Islands, related to the Ionian subduction.